

Electron Spin Resonance Studies of Anisotropic Rotational Reorientation and Slow Tumbling in Liquid and Frozen Media. III. Perdeuterated 2,2,6,6-Tetramethyl-4-piperidone *N*-Oxide and An Analysis of Fluctuating Torques¹

James S. Hwang, Ronald P. Mason, Llan-Pin Hwang, and Jack H. Freed*

Department of Chemistry, Cornell University, Ithaca, New York 14853 (Received September 16, 1974)

Publication costs assisted by the Petroleum Research Fund

A detailed analysis of line shapes and relaxation is made for the perdeuterated 2,2,6,6-tetramethyl-4-piperidone *N*-oxide (PD-Tempone) nitroxide radical covering the whole range from fast motional narrowing ($\tau_R \sim 10^{-12}$ sec) to the rigid limit ($\tau_R \sim 10^{-6}$ sec) in several deuterated solvents. The slow tumbling results show particularly good agreement with the slow tumbling theory of Freed, *et al.*, for a reorientational model of moderate jumps (*ca.* 50° rms), and essentially isotropic reorientation. It is shown that while such a model may not be readily distinguished, purely from its slow tumbling spectral predictions, from a free diffusion model including inertial effects, the latter model is incompatible with most other considerations. However, a simple analysis explicitly including the fluctuating (or random) torques indicates that more fundamental analysis of the dynamics may explain the slow tumbling results without necessarily involving substantial jumps. The spectral analysis is considerably enhanced by the increased resolution obtained from the use of the perdeuterated spin probe and deuterated solvents. Careful analysis of results at X-band and 35 GHz has shown that the nonsecular spectral densities exhibit significant deviations from a Debye-like spectral density yielding results very similar to those recently reported for the peroxyaminedisulfonate (PADS) radical. Related observations are discussed of apparent non-Debye-like spectral densities in the incipient slow tumbling spectra. These anomalies are also found to be amenable to a unified explanation in terms of the fluctuating torques. The analysis of much of the results in terms of a simple model yields an rms value for the fluctuating torques of *ca.* $\sqrt{6kT}$ and $\tau_M \sim \tau_R$ where τ_M is the relaxation time of the torques. The high-temperature electron-spin flip processes are consistent with a Hubbard-type spin-rotational mechanism, but the low-temperature results may be due to spin-rotational relaxation from intramolecular motions. The simple analysis of spin-rotational relaxation in terms of relaxation of the fluctuating torques is found to yield equivalent predictions to conventional treatments when the estimated values of rms torque and τ_M are used.

I. Introduction

In the earlier papers in this series, we have demonstrated the wide range of information which may be obtained from esr relaxation studies about rotational reorientation in liquids and frozen media when one carefully studies esr spectra over the full range from the very fast motional region to the rigid limit.² In particular, it was shown how the fast motional esr line widths, when carefully analyzed, yield very accurate values of the anisotropic rotational diffusion rates from the zero frequency or secular spectral densities,^{2a} while the nonsecular (microwave frequency) spectral densities may yield useful information about the frequency dependence of the rotational reorientational correlation functions, and these latter effects can to some extent be studied as a function of microwave frequency.^{2b} It was further shown how detailed analyses of the slow tumbling spectra (aided by extrapolation of the appropriate fast motional results) may be very effectively analyzed to demonstrate that the molecular motions significantly deviate from that of a Brownian motion model.^{2a} This is perhaps the only current experiment wherein a single experimental spectrum contains sufficient information to distinguish between different molecular models for rotational reorientation. Another source of useful information is saturation

studies, and in part II we have shown how these may be extended into the slow tumbling region.

The studies reported in parts I and II were all performed using the free radical peroxyaminedisulfonate (PADS). This radical was chosen because its esr spectrum contains enough structure to supply useful information, and, unlike the commonly used nitroxide spin labels, its spectra do not suffer from inhomogeneous broadening due to unresolved intramolecular proton interactions which can dominate the intrinsic line width.³ Accurate analyses for the interesting effects mentioned in the previous paragraph require, first of all, that well-resolved rigid limit spectra be obtained, from which it should be possible to directly measure the contributions from the magnetic tensors; and, furthermore, in the fast motional as well as the slow motional regions, the subtle relaxation features should not be obscured by the unresolved structure. On the other hand, the PADS radical is soluble only in water and aqueous glycerol, so it is not at all useful for studies of solvent-dependent effects. Also, it would be desirable to take advantage of the wide variety of nitroxide spin labels of different sizes and shapes in such studies. We have found that a significant step in the direction of carrying out accurate spin relaxation studies on (at least some) nitroxides may be achieved by the use of perdeuteration. We have synthesized the perdeuterated 2,2,6,6-tetramethyl-4-piperidone *N*-oxide (PD-Tempone) shown in Figure 1 by standard methods,⁴ and we have stud-

* Temporarily on leave at the Department of Physical Chemistry, Aarhus University, Aarhus, Denmark (Spring 1974).

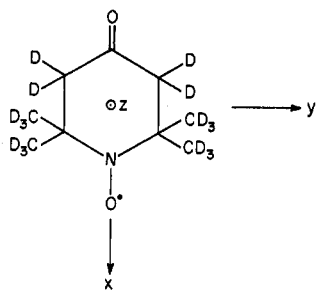


Figure 1. Perdeuterated 2,2,6,6-tetramethyl-4-piperidone *N*-oxide (PD-Tempone) showing molecular-fixed axis system.

ied its spin relaxation behavior in a variety of different solvents. We have been able to achieve accuracy comparable to that previously obtained with the PADS radical.² As will be shown below, the residual deuteron inhomogeneous broadening has only a marginal effect at most, and one may readily introduce small corrections to take care of these effects.

The undeuterated Tempone radical has been the subject of other investigations. Several esr analyses in the motionally narrowed region have been made.^{3,5,6} The conformation of Tempone has been crystallographically determined to be in a twisted boat conformation with the C=O and N-O bonds colinear, and, in the main, spherically symmetric. The bonds to the nitrogen atom lie approximately in a single plane.⁷ [In solution at room temperature interconversion between the two twisted boat conformations is either rapid and/or both methyl groups are at similar angles relative to the nitrogen $2p-\pi$ orbital because only one methyl ^{13}C hyperfine coupling constant of 5.7 G is observed.^{8a}] Our esr studies focus primarily on the orientation of the N-O fragment. Clearly the magnetic parameters associated with the \mathbf{g} tensor and the ^{14}N hyperfine tensor are the same in magnitude in the two identical twisted boat conformations, but (at least for the hyperfine tensor), shifted in orientation. Strictly speaking then, it is the reorientation of this N-O fragment (which could include a contribution from the interconversion if the rate of this process is not significantly slower than τ_R^{-1} , the overall reorientational rate) which is being studied in this investigation. One would, however, expect, that any residual contributions from intramolecular processes would obey very different dependences on viscosity and temperature than exhibited for the overall molecular reorientation.

We describe below the results of our studies with PD-Tempone. These results both amplify and support the earlier observations that were made on the PADS system. They also emphasize the importance of making accurate measurements of magnetic tensors, etc. in order that one can be confident of such features as anisotropic reorientation, model dependence, and non-Debye-like spectral densities. We note in particular that our results on the PD-Tempone system also confirm the nonsecular spectral densities previously seen with the PADS system, and other related anomalies are also reported which are associated with the pseudosecular and secular spectral densities. In an attempt to explain these spectral anomalies, we have considered a more detailed analysis of the molecular dynamics and have included explicit effects from the fluctuating or random torques acting on the Tempone probe. We also show how such an analysis could give new meaning to the slow-tumbling model-dependent observations.

II. Experimental Methods

Many of the experimental methods have been discussed in detail in parts I and II. We give below only the relevant additions and differences.

(A) *Preparation of Samples.* PD-Tempone was prepared by the method described by Rozantsev⁴ for Tempone. Perdeuterated acetone, ammonia, and hydrogen peroxide were used. NaOD was prepared from D_2O . The Trilon B and sodium tungstate were recrystallized three times from D_2O in order to further assure that every exchangeable proton was replaced by deuterium. Proton nmr in the manner of Kreilick^{8b} (of partially and completely deuterated Tempone) confirmed the absence of protons in PD-Tempone.

The perdeuterated toluene (Stohler Isotope Chemicals) was distilled under vacuum from a sodium mirror. The perdeuterated acetone (ICN) was used without further purification. The hydroxyl protons of glycerol (Matheson Coleman and Bell) were repeatedly exchanged with D_2O . The proton nmr of the 85% solution was free of all but a trace of the hydroxyl-water peak. The radical solutions ($1-10 \times 10^{-5} M$) were prepared with degassing on a vacuum line.

(B) *Computer Interfacing.* Line shape and line width analysis can be very time consuming without computer help. This is even more so for saturation measurements. Thus our spectrometers were interfaced with a PDP-9 computer. Since the output impedances of the two detection systems for E-12 and V4502 spectrometers are different, the former being low and the latter high, two interface units were built. We first describe the interfacing of the E-12 spectrometer.

The interface for the y axis of the E-12 spectrometer employs two differential amplifiers to provide high isolation from ground and to avoid loading the output of the E-12 spectrometer. For the x axis there is a choice of using either the square waves generated by the stepping motor of the E-80A recorder or the timer internal to the computer. We have chosen to use the latter because the full resolution in the x axis is not needed nor does the computer have enough memory (only 20K). We now discuss the y axis in greater detail. [The circuit diagram for the y axis is given in Appendix A.] We use for the input resistor a dual ten-turn 10-k Ω feedback resistor. The ten-turn pot can vary from 100 Ω to 10 k Ω giving a variable gain of 100. The output of the two amplifiers is not a floating output. One of the outputs is grounded at the AD converter such that the voltage is negative as required by the AD converter. A voltmeter helps the setting of the maximum gain for the signal. The basic interval of the timer used for the x axis is 1/60 sec so, for a 0.5-min scan, there are a maximum of 1800 points and a resolution of 0.06%. This is insignificant compared to the error of about 1% which is inherent in the spectrometer. To signal "start" and "stop" we used the same schematic as that of Gough,⁹ although we find that in most circumstances, the use of "start" provided by the start switch of the E-80A recorder is quite sufficient.

The phase sensitive detection system used for the V4502 spectrometer is a Keithley unit which has a 10-k Ω output impedance. The data acquisition amplifier¹⁰ we used for the Keithley unit is composed of three stages. In the first stage, the \pm terminals of the Keithley unit are connected to a differential input providing high isolation from ground. Two followers driving the inputs of a difference amplifier have been used (A and B), and the output is fed into common-mode rejection stage composed of C. Any signal common (*i.e.*, same phase and amplitude) is rejected by ap-

proximately 60 db. This stage also provides gain of approximately 100. Signal from C is sent to offset stage D which provides -5 V operating point so that the output of the interface fits on a 0 to -10 V scale required by the AD converter. Note that the time constant is given by RC where $R = 12.1$ k Ω and $C = 0.047$ μ F. This gives $\tau \sim 6 \times 10^{-4}$ sec. The offset of about -5 V is obtained from IR , where $I = 15$ V/36 k Ω and $R = 12.1$ k Ω . A schematic of the data acquisition amplifier is given in Appendix A.

The program for data collection and analysis is written in Fortran for the PDP-9 computer. The data collection is activated when the carriage hits the short switch. This gives a -10 V signal to the AD converter which is controlled by the ADREAD subroutine. This subroutine commands the AD converter to convert an analog voltage of a certain channel to a digital number, which will take about 40 μ sec, and provides the computer with this number. The timer is then started to run for 1/60 sec, then the channel for the y axis is read, and afterward the timer is stopped. This process is repeated for as long as the data points were collected. When all the data points are collected and dimensioned, they are smoothed by a least-squares procedure,¹¹ and the exact maxima are determined by fitting them to a quadratic or a cubic. The difference between the two maxima is the experimental line width. The scan is calibrated by using a TCNE sample which has a hyperfine splitting of 1.575 G.¹²

(C) *Line Width Measurements.* The line width and peak-to-peak heights obtained experimentally from the on-line analysis are stored in the Dectape which can then be used to analyze the data when the spectrometer is not in use (*e.g.*, while equilibrating between temperatures). The computer program for analyzing the data is written in such a way that one can use any one of the three line widths and all the three peak-to-peak heights to compute the three parameters A , B , and C in eq 1. The reason for doing this is that the error in the peak-to-peak heights is usually an order of magnitude less than that of the line widths. In order to utilize the peak-to-peak heights to compute the line widths, one must recognize that the line shapes are not strictly lorentzian in the presence of inhomogeneous broadening by the deuterons.^{3,13} The method for computing line widths from the peak-to-peak heights is described below.

From an analysis of the line shape it is possible to determine the deuteron hyperfine splitting, a_D , and this is done for each of the solvents used and their values are listed in Table I. The line shape analysis is performed at temperatures corresponding to minimum line widths. The computer simulation involves superimposing 25 equally spaced lines (spacing = a_D) of proper intensity distribution and of equal widths. It is then possible to determine a list consisting of three items, the "observed" line width, the "intrinsic" line width, and the "square root of the peak-to-peak height." In the computer memory, there are 450 arrays of these values, with the intrinsic line width ranging from 80 mG to 4 G. The computer compares the experimental line width with the list of 450 observed line widths and interpolates to give the corresponding values of the intrinsic width and peak-to-peak height. By taking the square root of the latter, we can obtain a proportionality constant for normalizing the two remaining experimental peak-to-peak heights. We can then use the same procedure to obtain the intrinsic line width except in this case we are starting from the peak-to-peak heights in order to obtain the corresponding "intrinsic" and "observed" line widths. The "observed"

line widths are printed in the output for comparison with the experimental values to make sure that they are within experimental error.

The three intrinsic line widths are fitted to the equation

$$\delta(M) = A + BM + CM^2 \quad (1)$$

where M is the spectral index number. The fractional errors in A , B , and C are also calculated in the computer analysis in the usual manner. The uncertainties in B and C are represented as error bars in the plot of C vs. B for PD-Tempone in toluene- d_8 , *cf.* Figure 3, and that of A in the plot of A' vs. τ_R , *cf.* Figure 5C.

(D) *T_1 Measurement.* The T_1 was measured by the continuous saturation method. We have measured T_1 as a function of temperature for PD-Tempone in toluene- d_8 and in 85% glycerol- D_2O . The standard procedure for measuring Q and hence the microwave magnetic field, B_1^2 , has been outlined in part II. The Q factor for both toluene- d_8 and 85% glycerol- D_2O are weakly increasing with decreasing temperature. The temperature ranges at which Q 's are determined are from 75 to -124° and from 30 to -62° , giving Q values of 7872 to 8104 and 7964 to 8653 for toluene- d_8 and 85% glycerol- D_2O . We have used two formats to determine T_1 . The first is the usual approach where line width squared is plotted as a function of microwave magnetic field squared and from the slope one gets the T_1/T_2 ratio and the intercept, T_2 . The second is to fix T_2 by measuring the line width in the absence of saturation. [The experimental line widths are all first corrected for inhomogeneous broadening due to the 12 deuterons as already described.] Our results indicate the second approach is more accurate. Also implicit in the measurement of T_1 is that the spin packets in the unresolved deuteron hyperfine structure are not significantly coupled to each other by any relaxation processes (*i.e.*, $W_e, a_D > W_D, \omega_{HE}$ where W_D is the deuteron spin-flip rate and ω_{HE} the Heisenberg exchange frequency), a condition that is readily satisfied if concentrations are kept low.

III. Results

A. Rigid Limit Simulations and Magnetic Parameters. Our rigid limit spectra and the best simulations for PD-Tempone in the different perdeuterated solvents are shown in Figure 2, and the magnetic parameters appear in Table I. The interpretation of line width studies in terms of the motion of PD-Tempone in solution depends directly on a determination of the hyperfine coupling tensor and g tensor in the particular solvent of interest. These parameters were, where possible, determined from spectra of PD-Tempone in an organic glass of a given solvent at temperatures low enough that the spectra were temperature independent. In the case of toluene¹⁴ and glycerol,¹⁵ it is known that there are no phase transitions in the viscous liquids over the temperature range of interest. Since acetone does not glass, only the magnetic parameters for the crystalline matrix could be determined.

The detailed assignments of the magnetic hyperfine and g tensor parameters are illustrated in Figure 2A. Note that in general it is possible to read off the values of A_z and g_z from the spectrum itself. However, a correct assignment of A_x and A_y , and g_x and g_y requires detailed spectral simulation.

The line width of the rigid limit spectra not only obscures the determination of the above magnetic parameters, but represents a variety of magnetic interactions

TABLE I: Magnetic Parameters

| | PD-Tempone ^o in toluene-d ₈ | PD-Tempone ^o in 85% glycerol-d ₃ -D ₂ O | PD-Tempone ^o in acetone-d ₆ | PD-Tempone ^o in ethanol-d ₆ | (a, p) | (b, q) | (c, r) | Tanol (d, s) | Tanane (d, t) |
|--------------------------|--|---|--|--|-----------------|----------------|------------------|-----------------|------------------|
| g_x | 2.0096 ± 0.0002 | 2.0084 ± 0.0002 | 2.0095 ± 0.0003 | 2.0092 ± 0.0004 | | 2.0089 ± 0.001 | 2.00783 ± 0.0002 | 2.0095 | 2.0103 |
| g_y | 2.0063 ± 0.0002 | 2.0060 ± 0.0002 | 2.0062 ± 0.0003 | 2.0061 ± 0.0004 | | 2.0058 ± 0.001 | 2.00604 ± 0.0002 | 2.0064 | 2.0069 |
| g_z | 2.0022 ± 0.0001 | 2.0022 ± 0.0001 | 2.0022 ± 0.0002 | 2.0022 ± 0.0003 | | 2.0021 ± 0.001 | 2.00270 ± 0.0002 | 2.0027 | 2.0030 |
| $\langle g \rangle^o$ | 2.0060 ± 0.00017 | 2.0055 ± 0.00017 | 2.0060 ± 0.00027 | 2.0058 _c ± 0.00037 | | | | 2.0062 | |
| g_s^f | 2.00602 ± 0.00005 | 2.00570 ₅ ± 0.00005 | 2.00598 ± 0.00005 | 2.00589 ± 0.00005 | 2.0062 ± 0.0002 | | | | |
| $z' = z$ | -4.68 ± 0.18 × 10 ⁻³ | -4.29 ± 0.18 × 10 ⁻³ | -4.63 ± 0.31 × 10 ⁻³ | -4.52 ± 0.43 × 10 ⁻³ | | | | | |
| $g(0)^k\{z' = y$ | 3.4 ± 1.8 × 10 ⁻⁴ | 3.6 ± 1.8 × 10 ⁻⁴ | 2.7 ± 3.1 × 10 ⁻⁴ | 2.6 ± 4.3 × 10 ⁻⁴ | | | | | |
| $z' = x$ | 4.38 ± 0.18 × 10 ⁻³ | 3.30 ± 0.18 × 10 ⁻³ | 4.31 ± 0.31 × 10 ⁻³ | 4.05 ± 0.43 × 10 ⁻³ | | | | | |
| $z' = z$ | 1.65 ± 0.1 × 10 ⁻³ | 1.2 ± 0.1 × 10 ⁻³ | 1.7 ± 0.2 × 10 ⁻³ | 1.6 ± 0.3 × 10 ⁻³ | | | | | |
| $g(2)^k\{z' = y$ | -3.7 ± 0.1 × 10 ⁻³ | -3.1 ± 0.1 × 10 ⁻³ | -3.7 ± 0.2 × 10 ⁻³ | -3.5 ± 0.3 × 10 ⁻³ | | | | | |
| $z' = x$ | 2.1 ± 0.1 × 10 ⁻³ | 1.9 ± 0.1 × 10 ⁻³ | 2.0 ± 0.2 × 10 ⁻³ | 2.0 ± 0.3 × 10 ⁻³ | | | | | |
| A_x, G | 4.1 ± 0.5 | 5.5 ± 0.5 | 4.8 ± 0.5 | 4.75 ± 0.6 | 5.2 | 5.8 ± 0.5 | 9.96 ± 1.07 | | |
| A_y, G | 6.1 ± 0.5 | 5.7 ± 0.5 | 5.4 ± 0.5 | 5.65 ± 0.6 | 5.2 | 5.8 ± 0.5 | 7.94 ± 1.07 | | |
| A_z, G | 33.4 ₃ ± 0.2 | 35.8 ± 0.3 | 34.0 ± 0.3 | { 15.43 ± 0.4 (66%) | 31 | 30.8 ± 0.5 | 32.6 ± 1.07 | | |
| $\langle A \rangle^i, G$ | 14.5 ₃ ± 0.4 | 15.7 ± 0.4 | 15.2 ± 0.4 | { 14.68 ± 0.4 (34%) | | | | | |
| a_N^f, G | 14.572 ± 0.015 | 15.740 ± 0.015 | 14.742 ± 0.015 | 15.173 ± 0.015 | | | | | |
| α^k | 1.2, ^m 2.15 | 1.8, 2.9 ^m | 2.45, 3.1 | 1.54 | | | | | |
| β^l | 0.2, 0.0 ^r | 0.3, 0.5 | 0.5, 0.7 | 0.0 | | | | | |
| $z' = z$ | 32.4 ± 0.4 | 34.4 ± 0.4 | 33.1 ± 0.4 | 34.2 ± 0.7 | | | | | |
| $\xi_N D^{(0)k}\{z' = y$ | -14.5 ± 0.9 | -17.2 ± 0.9 | -16.0 ± 0.9 | -16.3 ± 1.1 | | | | | |
| $z' = x$ | -17.9 ± 0.9 | -17.6 ± 0.9 | -17.1 ± 0.9 | -17.9 ± 1.1 | | | | | |
| $z' = z$ | -1.39 ± 0.7 | -0.105 ± 0.7 | -0.441 ± 0.7 | -0.631 ± 0.8 | | | | | |
| $\xi_N D^{(2)k}\{z' = y$ | 20.6 ± 0.5 | 21.2 ± 0.6 | 20.5 ± 0.6 | 21.3 ± 0.7 | | | | | |
| $z' = x$ | -19.1 ± 0.5 | -21.1 ± 0.6 | -20.1 ± 0.6 | -20.7 ± 0.7 | | | | | |
| a_D, mG | 20.5 ± 0.2 | 16.0 ± 0.2 | 22.4 ± 0.2 | 20.2 ± 0.2 | | | | | |

^aO. H. Griffith, D. W. Connell, and H. M. McConnell, *J. Chem. Phys.*, **43**, 2909 (1965). Tempone in toluene-d₈ and gaussian fit is best for PD-Tempone in 85% glycerol-D₂O. ⁿNote a W. L. Hubbell and H. M. McConnell, *J. Amer. Chem. Soc.*, **93**, 314 (1971). ^cS. Ohnishi, small β would help relative amplitude of $M_z = \pm 1/M_z = 0$ but give too much resolution in J. C. A. Boeyens, and H. M. McConnell, *Proc. Nat. Acad. Sci. U.S.A.*, **56**, 809 (1966). ^dD. central region. ^ePerdeuterated 2,2,6,6-tetramethyl-4-piperidone 1-oxyl. ^p2,2,6,6-Tetra-Bordeaux, J. Lalzerowicz-Bonneteau, R. Briere, H. Lemaire, and A. Rassat, *J. Org. Magn. methyl-4-piperidone 1-oxyl in tetramethyl-1,3-cyclobutadione crystal. q* N-Oxyl 4',4'-di-Resonance, **5**, 47 (1973). ^e $g = \frac{1}{2}(g_x + g_y + g_z)$. ^fMeasured in motionally narrowed region. methylloxazolidine derivative of 5- α -cholestan-3-one in cholesterol chloride. ^rNitroxide Error limits reflect total range of observed values. ^g $g^{(0)} = (6)^{-1/2}2g_z' - (g_z' + g_y')$ = maleimide spin-labeled horse oxyhemoglobin crystal. ^s2,2,6,6-Tetramethyl-4-piperidinol $\{3(6^{-1/2})g_z' - g_s\}$. ^h $g^{(2)} = \frac{1}{2}(g_x' - g_y')$. ⁱ $\langle A \rangle = \frac{1}{3}(A_x + A_y + A_z)$. ^j $\xi_N D^{(0)} = (\gamma_e/2\pi) \cdot 1$ -oxyl in crystal. ^t2,2,6,6-Tetramethylpiperidine 1-oxyl in crystal. ^uThese are the entries for $[2(6^{1/2})^{-1}2A_z' - (A_z' - a_N)]$ in megahertz. ^k $\xi_N D^{(2)} = \frac{1}{4}(\gamma_e/2\pi)(A_z' - A_y')$ in megahertz. ^vFor the two spectra. The respective values of $A_z(G)$ are 35.9 ± 0.4 (66%), 33.65 ± 0.4 (34%). ^lNumbers are for lorentzian and gaussian fit, respectively. ^mLorentzian fit is best for PD- and 35.1 ± 0.4 av.

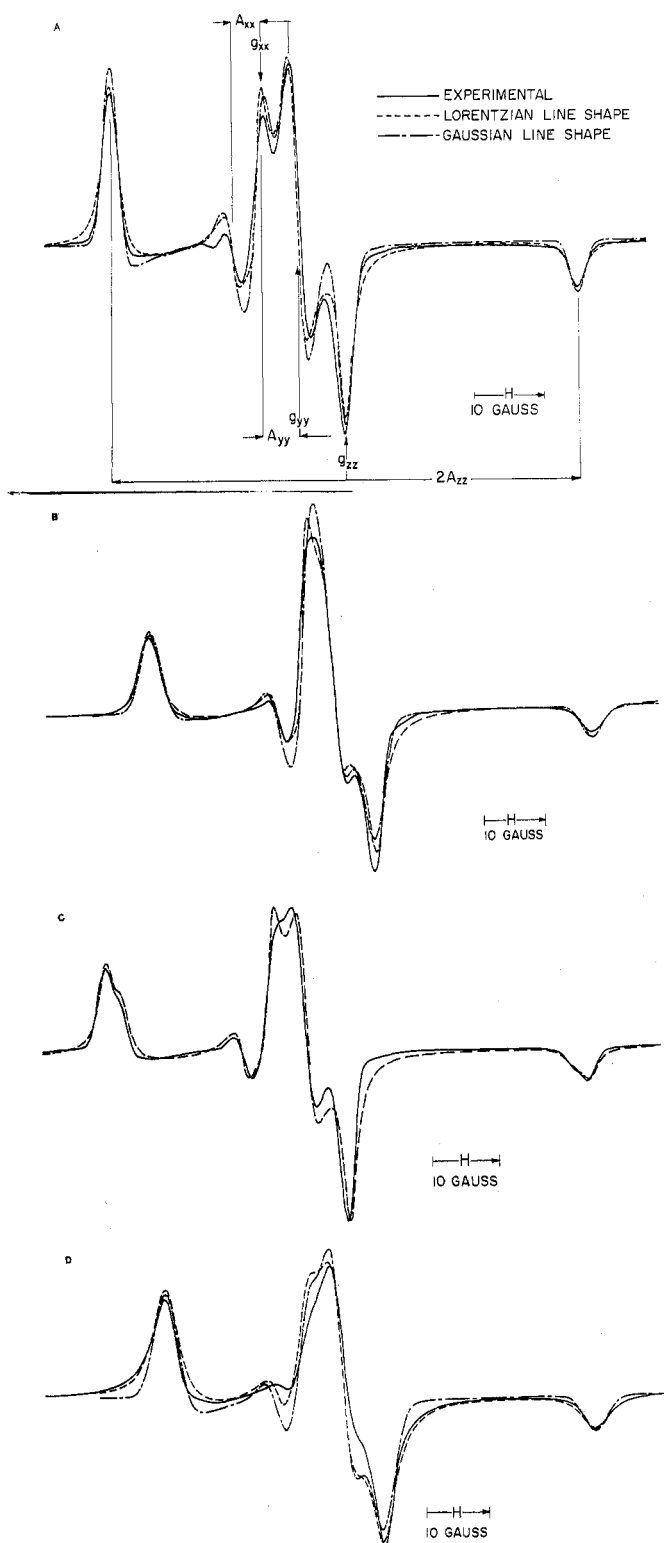


Figure 2. Rigid limit spectra for PD-Tempone and simulations based on magnetic parameters given in Table I. Solvents are (A) toluene- d_8 ; (B) glycerol- d_3 - D_2O ; (C) ethanol- d_6 ; (D) acetone- d_6 .

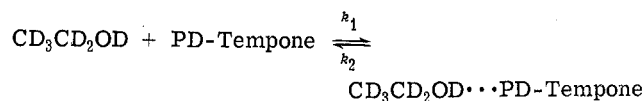
which would be very difficult to incorporate into theoretical line width expressions, except in a simplified form as a residual width. In order to reduce the rigid limit width due to intra- and interproton hyperfine interactions as much as possible, these studies were done with perdeuterated Tempone and perdeuterated solvents. The rigid limit spectrum in toluene- d_8 illustrated in Figure 2A had the lowest rigid

limit line width and was, therefore, most intensively studied.

The glycerol- d_3 - D_2O solvent also gave a well-resolved spectrum as shown in Figure 2B. Nitroxide radicals form hydrogen bonds, so the relatively large changes in appearance of these two spectra and the magnetic parameters derived from them is not unexpected. Note that only the change in g_x , A_x , and A_z is experimentally significant and that only the change in A_z exceeds the line width α .

The ratio of A_z to a_N was 2.30 and 2.28 in toluene- d_8 and glycerol- d_3 - D_2O , respectively. If solvent interactions reflected a change in the hybridization of the bonds about the nitrogen atom, a change in A_z/a_N would be expected.¹⁶

In Figure 2C one should note the inner humps on the outer hyperfine extrema which occur in the ethanol- d_6 glass. The two humps are readily interpreted as due to the existence of radicals with two different values of A_z . Detailed simulation leads to a value of 35.9 G for 66% of the radicals and 33.65 for 34%. A comparison of these two values with the values of A_z obtained in different solvents given in Table I leads us to believe that the lower value is characteristic of a nitroxide radical in the absence of hydrogen bonds (*i.e.*, A_z same as in toluene), while the higher value is characteristic of the PD-Tempone hydrogen-bonded solvent complex (*i.e.*, A_z same as in glycerol-water). An association constant for this equilibrium



can be calculated directly from the radical population ratio. Note that because the radical concentration, x , is much less than the bulk solvent concentration $[\text{CD}_3\text{CD}_2\text{OD}]$, $K = 0.66x/0.34 x [\text{CD}_3\text{CD}_2\text{OD} - x] = 2.0[\text{CD}_3\text{CD}_2\text{OD}]^{-1} = 0.12\text{L/M}$.

Note that the lifetime of these amphiphilic sites in the ethanol glass must be much longer than $(\gamma_e \Delta A_z)^{-1} \approx 2.5 \times 10^{-8}$ sec, where ΔA_z is the difference in A_z between the two distinguishable environments.

Nitroxide hydrogen-bonded solvent complex equilibria have been previously investigated in solution by the induced shifts of the solvent nmr spectra.^{17,18} The lifetime of a similar methanol nitroxide complex, k_2^{-1} , is estimated from nmr data to be 4×10^{-12} sec at room temperature.¹⁹ Note that the simulation of PD-Tempone in ethanol- d_6 in the region of the spectrum sensitive to g_x and A_x is too well resolved compared to the experimental result. This implies that two values of A_x and g_x , which are also solvent dependent, are actually present, although it does not appear possible to actually distinguish them through simulations.

Frozen acetone- d_6 solutions which were 5×10^{-3} M in PD-Tempone showed the generally broad lines associated with segregation of nitroxide radicals into clusters.²⁰ More dilute solutions, when frozen, were free of obvious radical association but still had a gaussian rigid limit peak-to-peak width of about 1 G wider than that found in the other solvents which glassed and were therefore free of crystallization-induced concentration of the solute. We may employ the well-known second moment expression,^{21a} $M_2 = 5.1\gamma^4 \hbar^2 S(S+1)/d^6$, where M_2 is the second moment and d is the distance between dipoles. The excess width, $M_2 \approx 0.5$ G,^{2b} would then correspond to an interelectron distance of 27 Å.

Because of the ambiguities associated with the acetone

and ethanol solvents the toluene- d_8 and glycerol- d_3 - D_2O systems were investigated most extensively.

All rigid-limit simulations of PD-Tempone, except the one for the ethanol- d_6 solvent, required an angular-dependent residual line width. As in previous work with PADS,^{2a} we assumed the simple form

$$X = \alpha + \beta \cos^2 \theta$$

where θ is the polar angle. The excess width of the outer hyperfine extrema could be due to a number of factors. One possibility is that a true rigid limit has not been reached, because the widths of these outer hyperfine extrema have been shown to be very sensitive to residual motion.^{21b} This possibility can probably be excluded by the observation that the apparent line width variation persists even at 20°K.^{22,23}

A possibly important contribution is unresolved intramolecular electron-host deuterium hyperfine structure. The A_z^D component of the methyl deuterium hyperfine tensor has been shown to be five times as great as A_{iso}^D or approximately 0.1 G.^{22,23} Note that even in toluene- d_8 , where the rigid limit width is narrowest, a lorentzian peak-to-peak width of 1.4 G is needed to simulate the outer hyperfine extrema, and would not be significantly further broadened by the 12 methyl deuteriums with a 0.1-G splitting. These considerations also apply to host deuterium hyperfine interactions, which may be large, especially in hydrolytic solvents where hydrogen-bonded nitroxide complexes are present (*i.e.*, $a_{EtOH}^H = -0.45$ G).¹⁷

In general, solvent perdeuteration, although responsible for noticeable reduction in rigid limit widths is much less effective than the ratio $I_{D\gamma D}/I_{H\gamma H} \sim 1/3$.²⁷ would imply.

It is clear that some other interaction must be present, which makes a major contribution to α , and is primarily responsible for β . In single crystal studies, where hydrogen host-electron dipole-dipole interaction is generally dominant,²⁴ each radical has an identical environment. In an unordered matrix local differences in solvent interactions appear to make an important contribution to the line width in these studies. (That is, one would have site variation in both the isotropic and anisotropic portions of g and A_z .) In the extreme case of ethanol- d_6 , two distinct populations of radicals represented by two A_z 's are present. Note that only in this case was it possible to get a good fit of the relative amplitudes of the outer hyperfine extrema to the central region of the spectrum without recourse to an orientation-dependent line width (*i.e.*, $\beta = 0.0$ G). If local variations in solvent interactions make a major contribution to α , then the observation that A_z is the most solvent dependent of the magnetic parameters would lead to an expectation of even larger widths for the outer hyperfine extrema which determine A_z , and, in extreme cases, a resolution of two A_z 's, as in the case of ethanol- d_6 where $\Delta A_z > \alpha$.

We also give in Table I the average values, g_S , a_N , and a_D from the motionally narrowed lines. The former two were measured by standard means,^{2a} while a_D was obtained by comparing the experimental line shape obtained in each solvent at that temperature yielding the narrowest intrinsic width (*i.e.*, displaying the greatest distortions from the inhomogeneous broadening due to the 12 methyl deuterium splittings), with computer simulations of the expected line shapes. The results were checked at several different temperatures and were not found to display any significant temperature dependences.

B. Line Width Results. 1. Motional Narrowing Region.

(a) *Toluene- d_8 Solvent.* The motional narrowing results have been analyzed in the standard manner.^{2a} The line width data are expressed in terms of eq 1. The theoretical expression for axially symmetric rotational diffusion is given by eq 5 of part I. A simpler form of this expression appropriate for isotropic rotational diffusion is given by Kooser, *et al.*²⁵ These expressions are based on Debye-type spectral densities for the nonsecular and pseudosecular terms.²⁶ As in part II, we have introduced an experimental adjustment parameter into the nonsecular spectral densities such that they are given by

$$j(\omega_0) = \tau_R / [1 + \epsilon \omega_0^2 \tau_R^2] \quad (2)$$

The Debye spectral densities are recovered by letting $\epsilon = 1$. The results of our experiments and analyses appear in Figures 3-8.

Our results for toluene- d_8 solvent, which was most extensively studied, are given as graph of C vs. B for both X band and 35 GHz in Figure 3. Our X-band results show constancy in the C/B ratio over the range of τ_R from 10^{-9} to $<10^{-10}$ sec. It has already been pointed out that this constancy is strong evidence against having any modulation process supplementary to the rotational diffusion contributing to the line width behavior.^{2a} Furthermore, we note that the experimental results can be fit with isotropic rotational reorientation (*i.e.*, if we let $N = R_{\parallel}/R_{\perp}$ then $N = 1$). The detailed analysis leading to this result is summarized in Table II. It is clear, however, that for $\tau_R \approx \omega_0^{-1} = 1.75 \times 10^{-11}$ sec, the experimental results deviate from the simple predictions and we must introduce the experimental adjustment factor ϵ that appears in eq 2. A value of $\epsilon = 5 \pm 1$ is seen to fit the experimental results at X band satisfactorily until about $\tau_R = 3 \times 10^{-12}$ sec. Our 35-GHz results are in good agreement with the values of τ_R and N from the X-band results. However, the large error in measuring C at the faster motions makes it impossible to determine an ϵ value from the 35-GHz C/B ratios. It may be seen from eq 5²⁷ of part I that B is more significantly affected by the nonsecular contributions. Thus, if the source of the deviation of the C/B ratio from that predicted by simple theory is due to the nonsecular terms, it should be possible to show that the primary source of the discrepancy arises from the observed values of B . This observation is illustrated in Figure 4A and B. Figure 4A gives the results of τ_R obtained from the X-band data as a function of η/T . The linear dependence of τ_R with η/T is clearly demonstrated in the 10^{-9} to 10^{-10} sec region. However, when $\epsilon = 1$ is utilized, then in the region τ_R of the order of 1.7×10^{-11} sec the values of τ_R obtained from B are seen to deviate significantly from a linear dependence on η/T , while those from C deviate only marginally. When $\epsilon = 5.4$ is utilized, then both sets of τ_R are seen to fall on the same extrapolated straight line.^{28a}

For $\tau_R \leq 3 \times 10^{-12}$ sec, the τ_R from B show only a small departure from the straight line extrapolation, while the τ_R from C show significant deviations. It is clear, therefore, that these deviations for the very fast motions, which are largely due to the anomalous behavior of C , may not be attributed to the same cause, *viz.* deviations of the nonsecular terms.

The 35-GHz results are analyzed in the same manner in Figure 4B. Here only the values derived from B are utilized, since we have already noted the values of C exhibit considerable experimental error. It is quite clear that these results are best fit with an $\epsilon = 5$. We finally note that from

TABLE II: Calculated C/B as a function of N^a for PD-Tempone^b in Different Solvents

| Toluene- d_8^b | | | | 85% glycerol- d_3 -D ₂ O ^c | | | | Acetone- d_6^d | | | |
|------------------|---|------------|-------------------|--|---------------------------------------|------------|-------------------|------------------|---|------------|-------------------|
| N | $(=0.925 \pm 0.016$ from experiment) | | | N | $(=1.18 \pm 0.02$ from experiment) | | | N | $(=1.082 \pm 0.003$ from experiment) | | |
| | C/B $z' = z^f$ | $z' = y^f$ | $z' = x^f$ | | C/B $z' = z^f$ | $z' = y^f$ | $z' = x^f$ | | C/B $z' = z^f$ | $z' = y^f$ | $z' = x^f$ |
| 6 | 0.985 | 1.40 | 0.726 | 6 | 1.23 | 1.77 | 0.911 | 6 | 1.04 | 1.65 | 0.731 |
| 3 | 0.956 | 1.12 | 0.792 | 3 | 1.20 | 1.43 | 1.00 | 3 | 1.01 | 1.26 | 0.818 |
| 1 | 0.925 | 0.925 | 0.925 | 1 | 1.17 | 1.17 | 1.17 | 1 | 0.986 | 0.986 | 0.986 |
| 1/3 | 0.901 | 0.858 | 1.02 | 1/3 | 1.16 | 1.08 | 1.28 | 1/3 | 0.971 | 0.873 | 1.11 |
| 1/6 | 0.890 | 0.839 | 1.05 ^e | 1/6 | 1.15 | 1.05 | 1.32 ^e | 1/6 | 0.965 | 0.868 | 1.15 ^e |

| Ethanol- d_6^e | | | | Toluene- d_8 (35 GHz) ^b | | | | A term in Gauss ^a ($\tau_R = 4 \times 10^{-10}$ sec) | | | |
|------------------|--|------------|-------------------|--------------------------------------|---|------------|--------------------|---|------------|------------|------------|
| N | $(=0.879 \pm 0.01$ from experiment) | | | N | $(=0.245 \pm 0.015$ from experiment) | | | N | | | |
| | C/B $z' = z^f$ | $z' = y^f$ | $z' = x^f$ | | C/B $z' = z^f$ | $z' = y^f$ | $z' = x^f$ | | $z' = z^f$ | $z' = y^f$ | $z' = x^f$ |
| 6 | 1.11 | 1.68 | 0.794 | 6 | 0.257 | 0.368 | 0.188 | 1.3 ⁱ | 0.5805 | 0.503 | 0.522 |
| 3 | 1.08 | 1.31 | 0.880 | 3 | 0.249 | 0.293 | 0.206 | 1 ⁱ | 0.512 | 0.512 | 0.512 |
| 1 | 1.05 | 1.05 | 1.05 | 1 | 0.241 | 0.241 | 0.241 | 1.3 ^j | 1.77 | 1.53 | 1.69 |
| 1/3 | 1.03 | 0.956 | 1.17 | 1/3 | 0.235 | 0.223 | 0.267 | 1 ^j | 1.59 | 1.59 | 1.59 |
| 1/6 | 1.02 | 0.931 | 1.20 ^e | 1/6 | 0.232 | 0.218 | 0.276 ^e | 1.5 ^k | 0.6701 | 0.534 | 0.556 |
| | | | | | | | | 1 ^k | 0.551 | 0.551 | 0.551 |

^a These values are calculated from eq 5 of ref. 2a, for the g and A values given in Table I for PD-Tempone in different solvents. It is assumed that $\omega_0^2 \tau_L m^2 \gg 1$ and $\omega_n^2 \tau_L m^2 \ll 1$. ^b Data analyzed using $N = 1$ and $\epsilon = 5.4$. ^c Data analyzed using $N = 1$ and $\epsilon = 1$. ^d Data analyzed using $z' = y$ with $N = 1.71 (\pm 0.02)$, and $\epsilon = 2.50$. ^e Data analyzed using $z' = x$ with $N = 3.02 (\pm 0.19)$, and $\epsilon = 3.33$. ^f z' is the symmetry axis of the diffusion tensor and x , y , and z are the molecular fixed axes (see text). ^g $\lim_{N \rightarrow 0} (C/B) = 1.08, 1.34, 1.17, 1.23$, and 0.284 for toluene- d_8 , 85% glycerol- d_3 -D₂O, acetone- d_6 , ethanol- d_6 , and toluene- d_8 (35 GHz), respectively. ^h Perdeuterated 2,2,6,6-tetramethyl-4-piperidone 1-oxyl. ⁱ These are values for toluene- d_8 solvent at X band. The experimental value is 0.57 ± 0.05 G. ^j These are values for toluene- d_8 solvent at 35 GHz. The experimental value is 1.9 ± 1 G. ^k These are values for 85% glycerol-D₂O solvent at X band. The experimental value is 0.68 G.

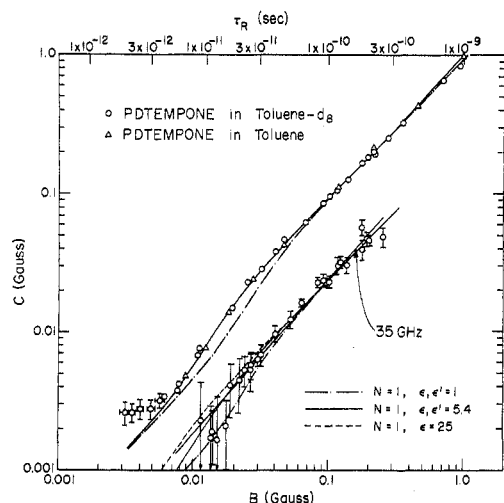


Figure 3. A comparison of experimental and calculated values of B vs. C for PD-Tempone in toluene solvents. The τ_R shown are for the X-band results. For 35 GHz, the correct τ_R values are those corresponding to the X-band experimental results with the same value for C as the 35-GHz results.

Figure 3 the B and C values are independent of whether toluene- d_8 or normal protonated toluene solvent is used.

We show in Figure 5A and B a summary of results for A vs. τ_R for X band and 35 GHz, respectively. For comparison, B and C (X band) are also shown. We also show the computed values for A (and B) from the dipolar and g tensor terms given in eq 5 of part I. We show in Figure 5C the

residual width A' representing the difference between the experimental A and the estimated A of Figure 5A and B as well as the A' for toluene- d_8 solvent. In the high-temperature region, this residual width A' should be primarily due to spin-rotational relaxation (cf. section IV). The high-temperature results for A' given in Figure 5C do indeed show the inverse dependence upon τ_R expected for spin-rotational relaxation and one notes the results for X band and 35 GHz are very nearly in agreement as they should be. (Small residual Heisenberg exchange effects may be contributing to the 35-GHz sample yielding the $\sim 10\%$ discrepancy.) However, for $\tau_R > 10^{-10}$ sec for X band and $\tau_R > 3 \times 10^{-10}$ sec for 35 GHz, A' begins to increase. We note, however, from Figure 5A and B that in this slower τ_R region the experimental values of A parallel those of B (and C) quite well just as they are predicted to, but they are about 10% higher for X band and 20% higher for 35 GHz than the estimated values. The residual width is outside the experimental uncertainty in measurement of the A and g tensors. The values given in Table I, lead to estimated error of 1.5–2% in computed A for X band and 3.5–4% for 35 GHz from this source in this region of τ_R .^{28b}

Actually one may suggest a possible explanation for this discrepancy between A and A' . It is noted from Table II that the B/C ratio is very insensitive to anisotropic rotation about the molecular z axis, so our results cannot really discriminate small anisotropies about this axis. However, we find that A (the dipolar and g tensor contributions) is very sensitive to anisotropic motion about the molecular z axis, but rather insensitive to anisotropic motion in which either

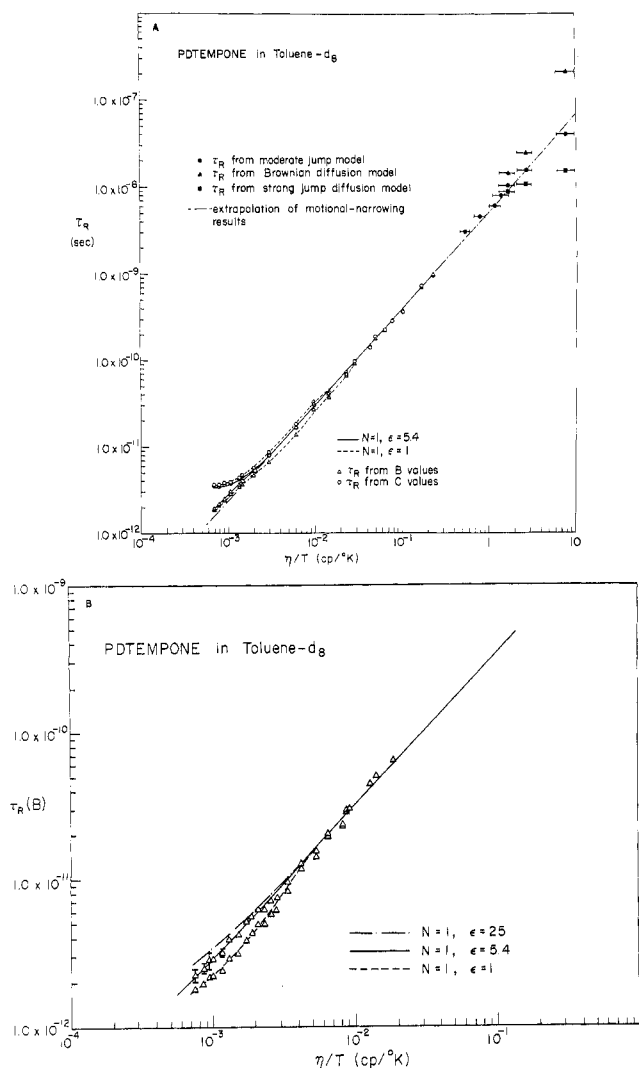


Figure 4. τ_R vs. η/T for PD-Tempone in toluene- d_8 solvent: (A) X-band; (B) 35 GHz.

the x or y axis is the principal axis. Thus if we let $N = 1.3$ with slightly faster motion about the z axis, then we can "explain" the total experimental A' (cf. Table II) for X band, and at least half the R-band A' , the latter being somewhat less certain.^{28b} (Note that an analysis of N based on the C/B ratio is generally not sensitive enough within experimental uncertainty to distinguish such small deviations from $N = 1$ about any axis.) Thus while there is not sufficient basis to assert that this is the explanation, it can very well be a major contributor to the small deviations between experimental and predicted A' for $\tau_R > 3 \times 10^{-10}$ sec.

We also show in Figure 5C, X-band results for toluene- h_8 solvent. The high-temperature A' 's are the same for toluene- d_8 and toluene- h_8 solvents. However, the low-temperature A' 's show distinct differences for the two solvents; that for the protonated solvent being somewhat larger. We discuss these observations on A' in section IV, but we note here that solvent interactions are clearly an additional source for the residual width A' .

(b) *Glycerol- d_3 Solvent.* The results for 85% glycerol- d_3 solvent appear in Figure 6A, B, and C. Here, because of the intrinsically greater viscosity, it was convenient only to study the region where $\tau_R \geq 10^{-10}$ sec. The C/B ratio is seen from Figure 6A to be constant over most of the range,

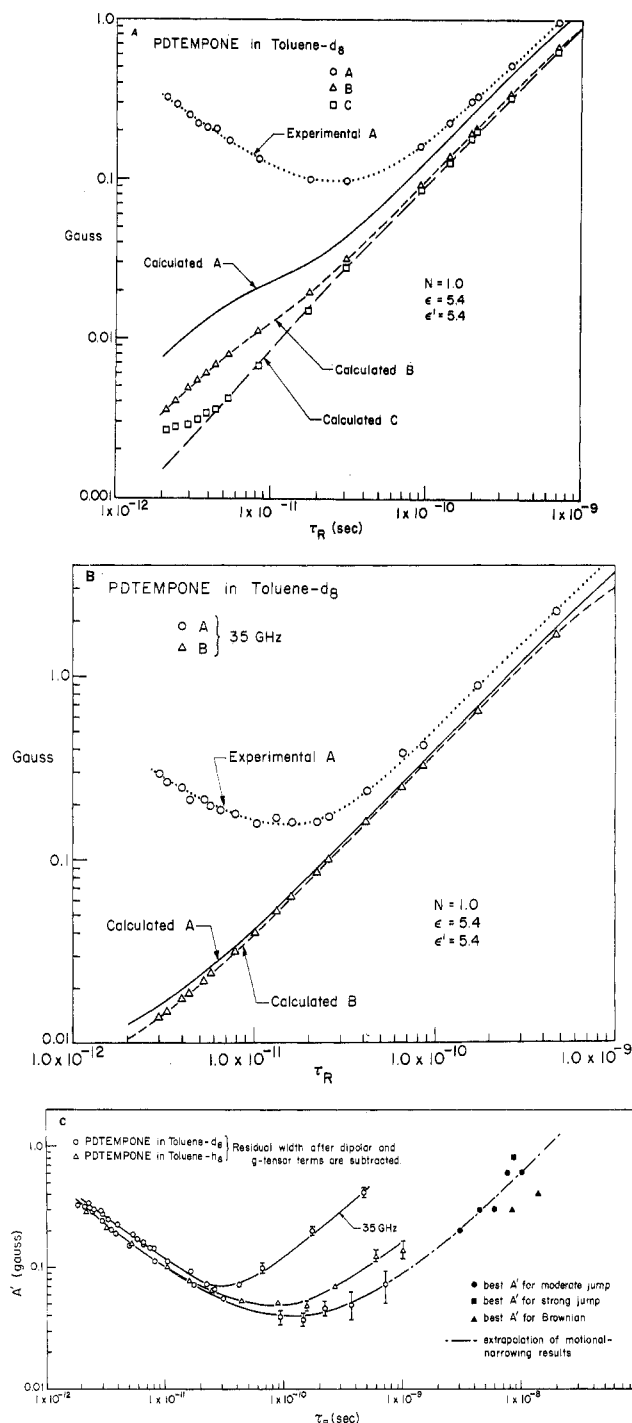


Figure 5. Comparison of experimental and calculated values of A' vs. τ_R for PD-Tempone in toluene solvents: (A) X-band; (B) 35 GHz. The calculated A' is from eq 5 of part I and includes only dipolar and g tensor contributions and neglects spin-rotational contributions. (C) $A' \equiv A_{\text{expt}} - A_{\text{calcd}}$ vs. τ_R .

but at $\tau_R \geq 5 \times 10^{-10}$ sec some discrepancy is observed. This discrepancy cannot be explained simply by corrections for slow tumbling which are found to almost be negligible in this region. Instead, by analogy with eq 2, one may try to fit the result to a modified pseudosecular spectral density given by

$$j(\omega_a) = \tau_R / [1 + \epsilon' \omega_a^2 \tau_R^2] \quad (3)$$

where ω_a is the ^{14}N , nmr resonant frequency, with the ex-

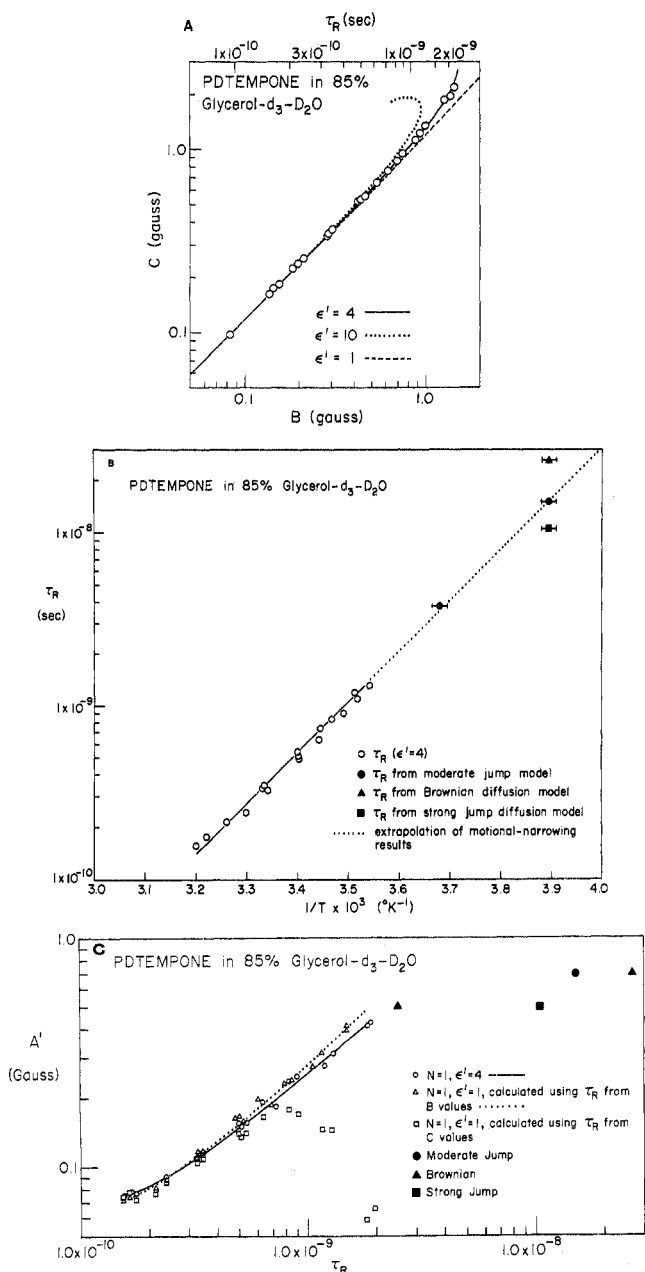


Figure 6. A comparison of the experimental and calculated A , B , and C values for PD-Tempone in 85% glycerol- d_3 - D_2O solvent: (A) B vs. C ; (B) τ_R vs. $1/T$; (C) A' vs. τ_R .

perimental adjustment parameter ϵ' . [Note that at $\tau_R = 10^{-9}$, $(\omega_a \tau_R)^2 \sim 1.7 \times 10^{-2}$, so any corrections to eq 3 are necessarily small.] However, because the anisotropic parameters given in Table I are comparable to ω_a , it turns out that the secular spectral densities may not either be considered simply as zero frequency terms. Both the secular and pseudosecular spectral densities must be corrected for residual effects of the anisotropic terms. We discuss these corrections in fuller detail in section V and Appendix C, where, in the context of a specific model for ϵ' , their nature is perhaps clearer. We note, also that in this region of τ_R , the high-field line is found to shift appreciably downfield. This is a dynamic frequency shift effect,^{29-32a} and the anomalously large shift can also be associated with the introduction of an $\epsilon' > 1$ (cf. section V and Appendix C).

The analysis in section V does lead to values of $\epsilon' \sim 4$ for

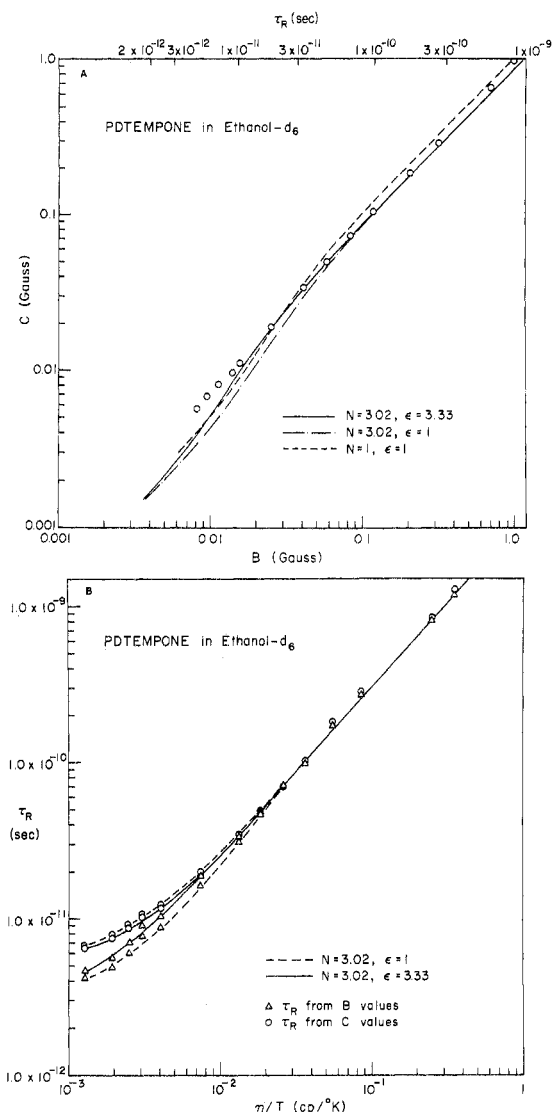


Figure 7. Experimental results and analysis for PD-Tempone in ethanol- d_6 solvent: (A) B vs. C ; (B) τ_R vs. η/T .

85% glycerol- d_3 solvent. (A careful analysis of the results in toluene solvent shows that for the magnetic parameters in this solvent, it is not possible to distinguish between $\epsilon' = 1$ or 4 either at X band or at 35 GHz, cf. Figure 3.) The results of such an analysis for the width contributions are shown in Figure 6A indicating the very good agreement obtained for the C/B ratio when $\epsilon' = 4$ vs. the unsatisfactory results if $\epsilon' = 1$ or 10. (The correct τ_R values predicted in this region are also somewhat dependent upon ϵ' . The values shown are for $\epsilon' = 4$.) The motional narrowing results of τ_R vs. $1/T$ in Figure 6B are shown for $\epsilon' = 4$. If we had instead used $\epsilon' = 1$, there would have resulted two distinctly different lines from the estimates of τ_R from the B and C values respectively. (Note that for glycerol solvent, it is generally preferable to plot τ_R vs. $1/T$ rather than η/T , cf. part I.)

The analysis of the dynamic frequency shifts is shown in Table III for several values of τ_R . It is seen how good agreement is achieved for the large decrease in the apparent hyperfine splitting between the center and high-field lines when $\epsilon' = 4$ is used instead of $\epsilon' = 1$.^{32b}

The residual component to A or A' is shown in Figure 6C

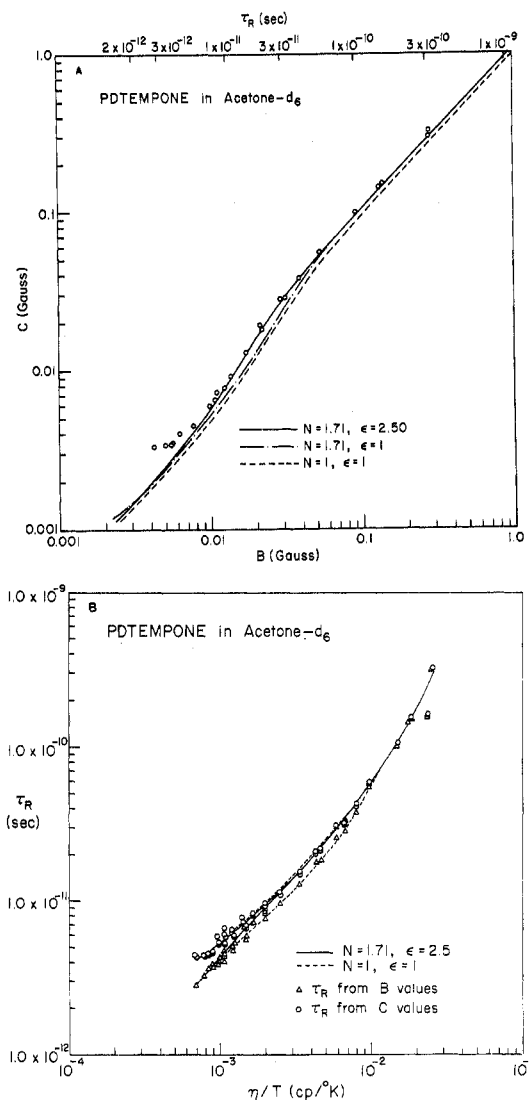


Figure 8. Experimental results and analysis for PD-Tempone in acetone- d_6 solvent: (A) B vs. C ; (B) τ_R vs. η/T .

for $\epsilon' = 1$ and 5. It is somewhat larger than the results in toluene solvent, but comparable to the results on the PADS radical in ice and glycerol- H_2O solvents (*cf.* parts I and II). One can again "explain" such a result by letting $N = 1.5$ with slightly faster rotation about the molecular x axis, but solvent interactions from the only partially deuterated solvent may be playing some role as well.

Note from Table II that from an analysis of C/B PD-Tempone appears to be rotating isotropically in glycerol solvent as well. The analysis and results summarized in Table II indicate how important it is to have accurate magnetic parameters before trying to determine anisotropic rotational diffusion from esr relaxation data. Thus, if for a moment we suppose the magnetic parameters of PD-Tempone had not been measured in glycerol solvent, and one chose to utilize the magnetic parameters obtained in toluene solvent, then the experimental C/B ratio of 1.18 would have been compared with the calculated ratios for toluene solvent. Then we would have obtained $N = 3.6$, with fastest rotation about the molecular y axis, instead of the isotropic result obtained with the correct magnetic parameters for glycerol solvent. (Of course our analysis of A suggests possible small anisotropies, but anisotropies of $N \sim 1.5$ are

TABLE III: Dynamic Frequency Shifts for PD-Tempone in 85% Glycerol- d_3 - D_2O Solvent

| $T, ^\circ C$ | τ_R, sec | Experimental ^a | | Calculated ^{a,b} | |
|---------------|-----------------------|---------------------------|-------------------|---------------------------|-------------------|
| | | $\Delta S_{1,0}$ | $\Delta S_{0,-1}$ | $\Delta S_{1,0}$ | $\Delta S_{0,-1}$ |
| 26.1 | 3.2×10^{-10} | 0.06 | -0.06 | -0.05 | -0.01 |
| | | | | (-0.05) | (0.01) |
| 15.3 | 8.4×10^{-10} | 0.05 | -0.23 | -0.05 | -0.26 |
| | | | | (-0.054) | (-0.12) |
| 11.2 | 1.1×10^{-9} | 0.05 | -0.47 | -0.05 | -0.47 |
| | | | | (-0.057) | (-0.23) |
| 5.8 | 1.36×10^{-9} | 0.08 | -0.73 | -0.06 | -0.70 |
| | | | | (-0.059) | (-0.366) |
| -1.15 | 3×10^{-9} | 0.09 | -2.63 | -0.15 | -2.53 |
| | | | | (-0.08) | (-1.74) |

^a $\Delta S_{1,0}$ is the difference in shift between the low-field and center lines; $\Delta S_{0,1}$ is the difference between the center and high-field lines. A positive (negative) ΔS means an apparent increase (decrease) in splitting compared to $a_N = 15.74$ G. ^b Calculated by method of Appendix C for $\epsilon, \epsilon' = 4$, while those in parentheses are for $\epsilon, \epsilon' = 1$.

within the range of uncertainty of our analysis of N from B/C .)

(c) *Ethanol- d_6 Solvent.* The results for ethanol solvent appear in Figure 7. The calculated results shown are based on the use of an average A_z as given in Table I. We are not able to fit these results with an isotropic rotational diffusion model. Our best estimate is $N = 3 \pm 1$ with fastest rotation about the molecular x axis, which seem reasonable (*cf.* section IV). This analysis is, of course, less certain, because of the existence of two different A_z values presumably due to the existence of two different species in the rigid limit. We can, however, compare results obtained using the average A_z with those obtained for the high value and the low value in Table I (presumably corresponding to the hydrogen bonded and nonhydrogen bonded species, respectively). For a typical result (at -4.7°) we would obtain values for N of 3, 3.5, and 2.2 respectively for the three cases. This would not be a substantial effect considering the uncertainty in our analysis. Note also from Figure 7A that the C/B ratio appears to increase somewhat at the longer τ_R in a manner very similar to the results in glycerol- d_3 solvent and may be explained in terms of an $\epsilon' > 1$. We note in this context that a proper determination of the parameters ϵ and ϵ' relies in part on a proper determination of N . Thus in part I, it was shown in an analysis of results on PADS that although ϵ is in principle affected by the use of an axially symmetric rotational diffusion model in place of a totally asymmetric model, that in practice such corrections would have only a marginal effect. We can, in the present case, compare the effects of using the three different A_z values with the associated N values obtained. In this example, we get values for ϵ of 3.4, 3.7, and 2.8, respectively. Thus the value of ϵ obtained is somewhat sensitive to typical variations in the magnitude parameters and the ensuing analysis. Note also from Figure 7B that for the faster motion (*i.e.*, $\tau_R \leq 10^{-11}$ sec) the values of τ_R obtained *vs.* η/T no longer fall on the extrapolated line that one would expect. While this is more dramatic for the τ_R values obtained from C , there is also a significant departure of the τ_R from values of B . This is to be compared with the result in toluene solvent and it probably indicates the onset of another relaxation process.

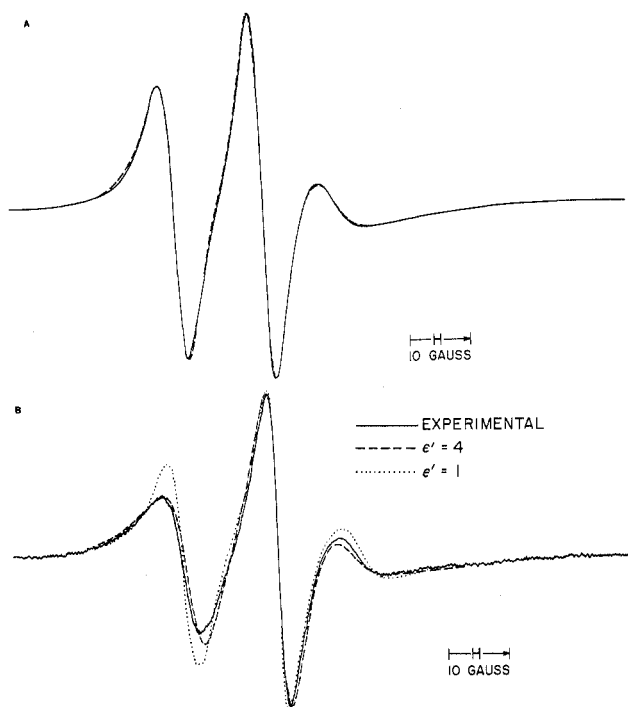


Figure 9. Comparison of experimental and simulated spectra in the incipient slow-tumbling region for PD-Tempone in (A) toluene- d_8 solvent ($\tau_R = 3.2 \times 10^{-9}$ sec) and (B) 85% glycerol- d_3 - D_2O solvent ($\tau_R = 3.8 \times 10^{-9}$ sec).

(d) *Acetone Solvent.* The results for acetone solvent appear in Figure 8. Here a slight deviation from isotropic rotation is suggested by the data, and the value for $\epsilon = 2.5$ is rather smaller than the result in the other solvents. In other respects the results are similar to those obtained in the other solvents.

2. Slow Motional Region. PD-Tempone was carefully studied in the slow motional region in both toluene- d_8 and glycerol- d_3 solvents. These spectra were analyzed in the same manner as in part I in terms of the slow tumbling theory of Freed, *et al.*²⁹ Typical experimental results and associated simulations are shown in Figures 9–11. One sees in Figure 9A the incipient slow motional region, $\tau_R = 3.15 \times 10^{-9}$ sec ($T = -112^\circ$) in toluene- d_8 solvent. This is a region, which typically is not very model sensitive, and we again find that a moderate jump model with an rms jump angle $\sim 50^\circ$ (which is equivalent in spectral predictions to a free diffusion model (*cf.* part I)) gives simulations virtually equivalent to a Brownian motion model. The agreement between theory and experiment is seen to be very nearly perfect. We show, in Figure 9B a similar result for PD-Tempone in 85% glycerol- d_3 - D_2O solvent utilizing a Brownian motion simulation. The agreement between experiment and prediction (for $\epsilon' = 1$) is not so good. The discrepancies are seen to be essentially the same as those already discussed for $\tau_R \sim 10^{-9}$ sec, *viz.* an incorrect C/B ratio and a large relative downfield shift of the high-field line. When adjustment is made for $\epsilon' > 1$ ($\epsilon' = 4$), then the results can be significantly improved as also shown in Figure 9B.

Figure 10 show results in the usual model-sensitive region,^{2a} $\tau_R \sim 10^{-8}$ sec. Here the experimental results in toluene- d_8 (Figure 10A) and in 85% glycerol- d_3 - D_2O (Figure 10B) are compared with the best simulations for Brownian diffusion, moderate jump diffusion, and strong jump diffu-

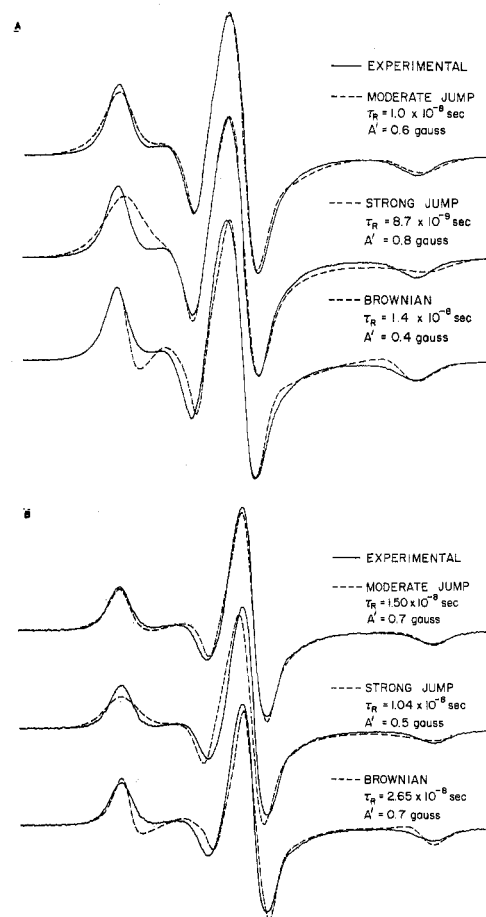


Figure 10. Comparison of experiment and simulated spectra in the model-dependent slow-tumbling region for PD-Tempone in (A) toluene- d_8 solvent and (B) 85% glycerol- d_3 - D_2O solvent.

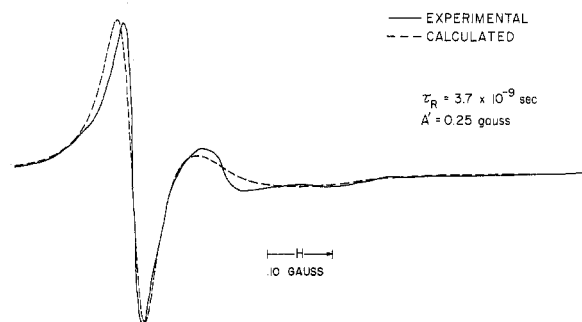


Figure 11. Slow tumbling spectrum for PD-Tempone in toluene- d_8 solvent at 35 GHz ($\tau_R = 3.7 \times 10^{-9}$ sec).

sion models^{2a} obtained by adjusting τ_R and A' . In the case of toluene- d_8 solvent, very good agreement is achieved for the moderate jump model, while the comparison is quite unsatisfactory for the other two models. This result is very similar, but with better agreement, to the PADS results in part I (where in the case of PADS adjustment had to be made for $N \neq 1$). The model dependence may also be studied by extrapolating the τ_R vs. η/T results from the motionally narrowing region into the slow motional region to compare with the best estimates obtained from the model-dependent studies. This has been done in Figure 4A, and one again sees the good agreement with the moderate jump diffusion model, but unsatisfactory results with the other models. (The results in Figure 5C for A' suggest that those

TABLE IV: Saturation Results for PD-Tempone in Toluene- d_8

| $T, ^\circ\text{C}$ | $10^{12} \tau_R, \text{sec}$ | $10^{-6} T_1^{-1}(0), \text{sec}^{-1}$ | $b^{a,b}$ | $10^{-6} W_e(0), \text{sec}^{-1}$ | $T_1^{-1}(-1)/T_1^{-1}(0)^c$ | $T_1^{-1}(+1)/T_1^{-1}(0)^c$ | | |
|---------------------|------------------------------|--|-----------|-----------------------------------|------------------------------|------------------------------|-------------------------|-------------------------|
| 80.4 | 2.44 | 3.89 ^d | 0.00538 | 0.00538 | 1.90 | 1.90 | 1.02 ± 0.05(1.00, 1.00) | 0.97 ± 0.04(1.02, 1.01) |
| 51.0 | 3.43 | 2.89 ^d | 0.0104 | 0.0104 | 1.37 | 1.38 | 1.07 ± 0.04(1.00, 1.00) | 0.98 ± 0.04(1.03, 1.02) |
| 19.2 | 5.50 | 1.96 ^d | 0.0264 | 0.0259 | 0.871 | 0.886 | 1.02 ± 0.04(1.00, 0.99) | 1.13 ± 0.04(1.06, 1.04) |
| -1.7 | 7.96 | 1.59 ^d | 0.0516 | 0.0492 | 0.644 | 0.676 | 0.97 ± 0.05(0.99, 0.97) | 1.09 ± 0.05(1.10, 1.04) |
| -34.5 | 17.6 | 1.00 ^d | 0.319 | 0.230 | 0.231 | 0.320 | 1.04 ± 0.06(0.91, 0.87) | 1.24 ± 0.08(1.14, 0.95) |
| -50.0 | 31.0 | 0.91 ^d | 1.28 | 0.565 | 0.101 | 0.229 | 0.84 ± 0.06(0.78, 0.80) | 1.08 ± 0.06(1.00, 0.85) |
| -50.9 | 31.0 | 1.05 ^d | 0.775 | 0.446 | 0.167 | 0.290 | 0.76 ± 0.10(0.81, 0.82) | 0.91 ± 0.08(0.99, 0.86) |
| -61.3 | 46.1 | 1.04 | 1.52 | 0.772 | 0.127 | 0.249 | 0.75 ± 0.12(0.75, 0.79) | 0.85 ± 0.12(0.89, 0.82) |
| -72.2 | 74.1 | 1.08 | 2.42 | 1.33 | 0.128 | 0.233 | 0.77 ± 0.12(0.75, 0.79) | 1.05 ± 0.17(0.84, 0.81) |
| -76.7 | 91.3 | 0.988 ^d | 3.67 | 1.95 | 0.104 | 0.195 | 0.70 ± 0.05(0.76, 0.80) | 0.97 ± 0.09(0.84, 0.81) |
| -81.9 | 123 | 0.851 | 6.30 | 3.30 | 0.0816 | 0.156 | 0.86 ± 0.16(0.80, 0.83) | 0.83 ± 0.12(0.86, 0.85) |
| -86.2 | 163 | 0.967 | 5.65 | 3.88 | 0.120 | 0.161 | 0.82 ± 0.08(0.83, 0.85) | 0.99 ± 0.15(0.87, 0.86) |
| -89.8 | 217 | 0.799 ^d | 9.52 | 6.59 | 0.0950 | 0.133 | 0.70 ± 0.07(0.88, 0.89) | 0.51 ± 0.05(0.90, 0.89) |
| -91.8 | 238 | 0.834 | 9.44 | 6.91 | 0.105 | 0.139 | 0.84 ± 0.18(0.88, 0.89) | 0.73 ± 0.22(0.90, 0.90) |
| -92.6 | 278 | 0.623 | 16.7 | 11.2 | 0.0695 | 0.103 | 0.98 ± 0.13(0.92, 0.92) | (0.93, 0.93) |

^a $b = W_N/W_e(0)$ where $2W_N$ is the nuclear spin-flip rate. ^b Numbers are calculated utilizing $\epsilon = 1$ and 5.4, respectively. ^c Numbers in parentheses are calculated from eq 4.1 of ref 2b utilizing $\epsilon = 1$ and 5.4, respectively. ^d $T_1^{-1}(0)$ calculated using slope and intercept method, see text.

for the moderate jump model are preferred, but they are not very conclusive.)

Similar comments apply to the model-dependent study for glycerol- d_3 - D_2O solvent in Figure 10B, except the predicted model-dependent line shape variations are somewhat less pronounced in this case, but the agreement is clearly best with a moderate jump model. The comparison with extrapolated τ_R vs. $1/T$ results in Figure 6B also favors moderate jump, although the result is a little more ambiguous because of the effects of ϵ' on the motional narrowing results, and the fact that τ_R need not exhibit a simple $1/T$ behavior (cf. part I). [It should be noted that the model-dependent results of Figure 10B were simulated with $\epsilon' = 1$, cf. section V.]

We have also examined the slow tumbling spectrum (in toluene- d_8 solvent) at 35 GHz. A typical experimental result (with the computer simulation) $\tau_R = 3.7 \times 10^{-9}$ sec is shown in Figure 11. One may compare this figure with Figure 9A, the X-band spectrum at nearly the same τ_R . It is clear that at 35 GHz, one is observing more of a slow motional spectrum. That is, because the g tensor contribution to the spin Hamiltonian is about four times greater (and $C \approx B$ at X band), the slow motional region is found to begin at $\tau_R \geq 0.25 \times 10^{-9}$ sec at 35 GHz compared to $\tau_R \geq 10^{-9}$ sec at X band. However, other features at 35 GHz, resulting from the greater importance of the g tensor, make it less desirable for study. First, as is clear from Figure 11, only the low-field portion of the spectrum is well resolved. The high-field portion is broadened out by effects akin to an enlarged B term (as well as A term) in eq 1. Thus, less of the spectrum is suitable for comparison with simulations. Secondly, the well-defined portion of the spectrum is more dependent upon the accuracy of the g tensor values, which are usually less accurate than those of A (cf. Table I). Thus, the agreement in Figure 11 between prediction and experiment is not as good as obtained for X band, and this problem increases as the motion slows further. For these reasons the analysis of the 35-GHz slow-tumbling results was not carried further.

C. Saturation Studies. Temperature-dependent T_1

studies were performed in the motional narrowing region for PD-tempone in toluene- d_8 solvent and also in glycerol solvent. The analysis of the results is identical with that given in part II. We present in Table IV the results of the detailed analysis for the extensive experiments performed in toluene- d_8 solvent. In particular, it is shown how the different choices for ϵ affect the different parameters. It was pointed out in part II that the ratios of the T_1 's for the different hyperfine lines could, in principle, provide a test for ϵ . However, we again find (as in part II), that the measurements are not accurate enough. In fact, as a result of the residual inhomogeneous broadening by the deuterons, we find somewhat greater experimental error in the present case for these ratios.

However, we note from Table IV that the values of W_e (and $b \equiv W_N/W_e$) are substantially affected by the choice of ϵ , deviating by as much as a factor of 2 for $\epsilon = 1$ vs. 5.4. The W_e results with $\epsilon = 5.4$ are plotted in Figure 12. The results in glycerol solvent as well as the results on PADS given in part II are also shown. The low viscosity T_1 results corresponding to $\tau_R < 10^{-11}$ sec are found to be roughly linear in τ_R^{-1} , but for $\tau_R > 10^{-11}$ sec the W_e results show a much weaker dependence on τ_R^{-1} of the order $\tau_R^{-1/3}$ for the results on PD-Tempone and $\tau_R^{-1/4}$ for the PADS results. This overall lack of simplicity of the dependence of W_e on τ_R^{-1} does not permit an unambiguous choice between the W_e 's calculated for the two different ϵ values, but those for $\epsilon = 5.4$ are somewhat favored. However, our results obtained from continuous saturation in conjunction with either (1) saturation recovery experiments in which W_e is measured directly,³³ or (2) elder experiments in which b is measured directly^{34,35} should permit a distinction to be made between the ϵ values. (The results for PADS in part II do not display nearly so sensitive a dependence of these parameters on the value of ϵ . This is because the values of b for a given τ_R value are somewhat larger in the present case. This has the effect of increasing the relative importance of the nonsecular dipolar contribution to T_1 compared to spin-rotation-type terms.) We have found that the W_e determination is not very sensitive to ϵ' , be-

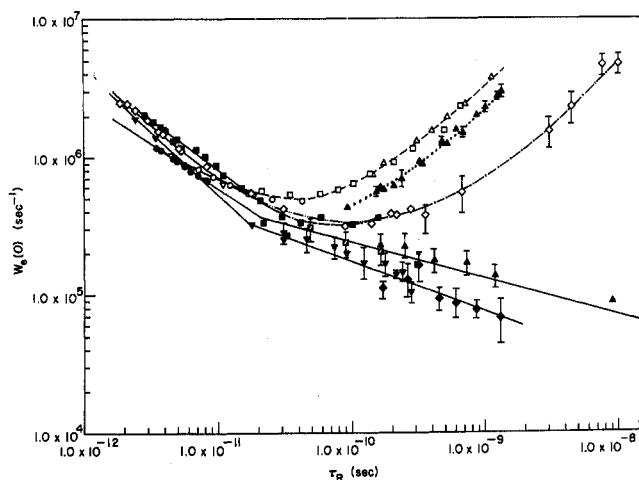


Figure 12. W_e vs. τ_R in various solvents. $W_e = \sqrt{3/4} \gamma_e A'$: (\diamond) PD-Tempone in toluene- d_8 , (\blacktriangle) PD-Tempone in 85% glycerol- d_3 - D_2O , (\blacksquare) PD-Tempone in acetone- d_6 , (\bullet) PADS in H_2O , (∇) PADS in 10% glycerol- H_2O , (\circ) PADS in 30% glycerol- H_2O , (\square) PADS in 50% glycerol- H_2O , (\triangle) PADS in 85% glycerol- H_2O . W_e calculated from T_1 : (\blacktriangledown) PD-Tempone in toluene- d_8 , (\blacklozenge) PD-Tempone in 85% glycerol- d_3 - D_2O , (\bullet) PADS in H_2O , (\boxtimes) PADS in 50% glycerol- H_2O , (\blacktriangle) PADS in 85% glycerol- H_2O .

cause corrections for ϵ' are important only in the region where $b \gg 1$, so that $W_e \approx (6T_1)^{-1}$ is virtually independent of b .

We also show in Figure 12 the line width parameter $1/2 A'$ for comparison. It is seen that for $\tau_R < 10^{-11}$ sec; the W_e estimated in the two ways are virtually identical, as expected for spin rotational relaxation, but for $\tau_R > 10^{-11}$ sec the two kinds of results show markedly different behavior, as would be expected if A' is due to small uncertainties in the value of N , solvent interactions, etc. The high-temperature values for A' taken as given by

$$A' \equiv A_1^2 \tau_R^{-1} \quad (4)$$

lead to experimental results for the coefficient A_1^2 which are shown in Table V. They are also compared with theoretical predictions, cf. section IV, and with recent results on VOAA.³⁶

IV. Further Discussion

A. Rotational Diffusion. Effective Rotational Radii. We can, from the slopes of the graphs of τ_R vs. η/T obtain estimates of the effective rotational radii utilizing a Stokes-Einstein relation

$$\tau_R = \frac{4}{3} \frac{\pi r_e^3 \eta}{kT} \quad (5)$$

where r_e is the effective rotation radius. These results are shown for this work and for the PADS results in Table VI. The experimental estimates are seen to be consistently smaller than the values calculated from geometric considerations. The geometric results are based upon values of $a_x \cong 4.2$ Å, $a_y \cong 2.7$ Å, $a_z \cong 3.0$ Å for Tempone⁷ and $a_x = 2.2$ Å, $a_y = 2.9$ Å, $a_z = 1.8$ Å for PADS.³⁷ Thus the shapes of both of these molecules are nearly prolate axially symmetric ellipsoids with the long axis a_{\parallel} and short axes a_{\perp} , such that $a_{\parallel} = a_x = 4.2$ Å and $a_{\perp} \cong 2.85$ Å for PD-Tempone and $a_{\parallel} = a_y = 2.9$ Å and $a_{\perp} \cong 2.0$ Å for PADS. One may readily predict R_{\parallel} and R_{\perp} from these dimensions for a Stokes-Einstein model. One has³⁸

TABLE V: Analysis of Residual Line Widths A' ^a

| | A_1^2 in 10^{-13} G sec ^b (from g values) | A^2 in 10^{-13} G sec ^c |
|---------------------------------------|---|--|
| PD-Tempone in toluene- d_8 | 4.99 | 6.12 |
| PD-Tempone in toluene | 4.99 | 6.6 |
| PD-Tempone in 85% glycerol- D_2O | 3.76 | |
| PD-Tempone in acetone- d_6 | 4.87 | 9.96 |
| PD-Tempone in ethanol- d_6 | 4.53 | 6.65 |
| PADS in ^d glycerol- H_2O | 3.16 | 3.10 |
| PADS in ^e frozen H_2O | 3.26 | |
| VOAA in ^f toluene | 319 | 320 |
| VOAA in ^g ethanol | 319 | 1268 |
| VOAA in ^h 1-propanol | 319 | 1960 |
| VOAA in ⁱ 2-propanol | 319 | 2001 |

^a Table based upon the fits of the residual A' to eq 4. ^b Calculated from spin-rotational contribution to $A' = \sum_i (g_i - g_e)^2 / 9\tau_R \equiv A_1^2 \tau_R^{-1}$. ^c Obtained by least-squares fits of results to eq 4. ^d From ref 2b. ^e From ref 2a. ^f From ref 36. ^g N. S. Angerman and R. B. Jordan, *J. Chem. Phys.*, 54, 837 (1971).

TABLE VI: Effective Rotational Radii

| System | Slope, ^a sec ² K p ⁻¹ | r_e , Å ^b | r_e , Å (geo- metric) ^c |
|---------------------------------------|---|---------------------------|---|
| PD-Tempone in toluene- d_8 | 4.03×10^{-7} | 2.37 | 3.2 |
| 85% glycerine- D_2O | (1.33×10^{-7}) | 1.64 | |
| Acetone- d_6 | 5.07×10^{-7} | 2.56 | |
| Ethanol- d_6 | 3.29×10^{-7} | 2.21 | |
| PADS ^d in glycerol- H_2O | | 1.16 | 2.2 |
| H_2O | | 1.49 | |

^a Slopes are from Figures 4B, the data of 6B plotted vs. η/T , 7B, and 8B. ^b Estimated from the slope and eq 5. ^c Estimated from X-ray dimensions, see text. ^d From ref 2b.

$$R_i = kT/8\pi\eta a_{\parallel}^3 \sigma_i \quad i = \parallel \text{ or } \perp \quad (6)$$

where

$$\sigma_{\parallel} = \frac{2}{3} \lambda^2 (1 - \lambda^2) \left[1 - (1 - \lambda^2) \lambda^{-1} \ln \frac{1 + \lambda}{[1 - \lambda^2]^{1/2}} \right]^{-1} \quad (7)$$

and

$$\sigma_{\perp} = \frac{2}{3} \lambda^2 (2 - \lambda^2) \left[(1 + \lambda^2) \lambda^{-1} \ln \frac{1 + \lambda}{[1 - \lambda^2]^{1/2}} - 1 \right]^{-1} \quad (8)$$

with $\lambda = (a_{\perp}^2 - a_{\parallel}^2)^{1/2} / a_{\parallel}$ and $0 < \lambda \leq 1$. One obtains $\sigma_{\parallel} = 0.402$ and $\sigma_{\perp} = 0.543$ for PD-Tempone and virtually the same result for PADS but with the different symmetry axis. The results in Table VI are given by $r_e = 1/3 [\sigma_{\parallel}^{1/3} + 2\sigma_{\perp}^{1/3}] a_{\parallel}$, which differs only slightly from the simple mean values.

However, eq 6–8 lead to the prediction of an $N = R_{\parallel}/R_{\perp} = 1.35$, *i.e.*, only a small asymmetry in the rotational diffusion. This estimate is consistent, within experimental error, with our observations that $N \cong 1$ for PD-Tempone in toluene and glycerol solvents. However our result for ethanol solvent implies somewhat faster rotation about the $a_{\parallel} = a_x$ axis, $N \approx 3$. This latter result is more characteristic of the observations for PADS in D₂O and glycerol of $N \approx 3$ and 4.7, respectively. These experimental results are clearly not consistent with the simple geometric considerations and may well be due, in the case of PADS, to strong interactions of the charged SO₃⁻ groups with the surrounding solvent. The case of PD-Tempone in ethanol may reflect strong H bonding tendencies, such as those indicated by the rigid limit spectra, showing, what we have interpreted as two species, one with a hydrogen bond and one without. The general availability of hydroxyl protons for H bonding is much less in ethanol than in glycerol–H₂O. Thus a given H bond of the nitroxide may persist longer in the case of ethanol, thereby creating a somewhat anisotropic motion.

One may choose to interpret the difference between the calculated r_e and the experimental values in terms of a microviscosity or an effective slip such that $r_e^3 \equiv \kappa r_0^3$ with r_0 the hydrodynamic radius and $0 \leq \kappa \leq 1$.³⁹ One would then get values of κ ranging from 0.13 in the glycerol solvents to 0.4 in toluene (or 0.5 in the less certain case of acetone), and κ would necessarily be independent of η/T from our experimental results. The low values for κ , both for PD-Tempone and PADS in the glycerol solvents, are consistent with the usual picture of a highly structured liquid with clathrate-type vacancies.

Our results may be compared to those on VOAA³⁶ for which $r_0 = 3.8$ Å from translational diffusion measurements,⁴⁰ but $r_0 = 3.4$ Å from X-ray structure,⁴¹ while r_e is found to range from 3.0 to 3.8 Å in different solvents, with the lower values typically for the non-H-bonding solvents and the higher values for H-bonding solvents. Thus the VOAA complex shows less hydrodynamic slip than the nitroxides, and a greater anisotropic intermolecular interaction for H-bonding solvents.

B. Spin Rotational Relaxation. W_e and A' . It is seen that the experimental estimates of A_1^2 defined by eq 4 and tabulated in Table V and of W_e in Figure 12 are generally in reasonably good agreement with the simple estimate of the spin-rotational contribution to A'^2

$$A'^{\text{SR}} = 2W_e^{\text{SR}} = \sum_i (g_i - g_e)^2 / 9\tau_R \quad (9)$$

where we have used the Hubbard-type relation:⁴³

$$\tau_J = (I/6kT)\tau_R^{-1} \quad (10)$$

There is a general trend, however, for the experimental values of A_1^2 for VOAA in H-bonding solvents to be somewhat larger, and this has already been noted.³⁶ Our results for PD-Tempone in ethanol-*d*₆ appear to show a similar discrepancy. But the generally good $\tau_R^{-1} \propto T/\eta$ dependence of A' at higher temperatures should still imply a spin-rotational relaxation mechanism even if the exact dynamical model is less certain (see discussion in section C about jump models).

One may estimate values of τ_J from eq 10. The moments of inertia I_x , I_y , and I_z for PD-Tempone are estimated to be 1.01, 1.10, 1.50×10^{-37} g cm², respectively, from molecular dimensions, yielding an average I of 1.20×10^{-37} g cm². Then

$$\tau_J = 1.45 \times 10^{-22} (\tau_R T)^{-1} \text{ sec} \quad (11)$$

Thus for $\tau_R \sim 10^{-11}$ sec (and $T \sim 270^\circ\text{K}$) where the W_e curves change over from linear in τ_R^{-1} to a weaker dependence upon τ_R^{-1} , one has $\tau_J \sim 5.4 \times 10^{-14}$ sec, with even shorter values for $\tau_R > 10^{-11}$ sec. Such values are already of the order of, or faster than molecular vibrational periods. Thus, one can question the interpretation and physical meaning of τ_J , when it becomes comparable to or faster than τ_M , the correlation time for the fluctuating (anisotropic) intermolecular potentials. This matter is discussed in section V.

It is still necessary to consider the low-temperature W_e 's which do not exhibit simple dependence on τ_R^{-1} . There exist, however, some nmr observations on T_1 , which bear some similarities to our observations on the lower temperature results for W_e . It has been found in several nmr studies that at lower temperatures, the presumed spin-rotational T_1^{-1} contribution becomes more nearly temperature and viscosity independent, and this has been attributed to spin-rotational relaxation due to internal rotational motions.⁴⁹ Such a possibility could exist in the present case in particular for PD-Tempone, for which there is likely to be an interconversion between the two equivalent twisted boat conformations which affects the orientation of the N–O fragment, as already noted in the Introduction.⁵⁰ The K₄(PADS)₂ dimer appears from an X-ray study to be approximately planar.³⁷ However, it may be that the PADS²⁻ anion could show a small nonplanarity with an interconversion between the equivalent forms. As in the nmr case,⁴⁹ experiments as a function of pressure would help distinguish between solvent-dependent overall reorientations and internal rotational effects due to the significant pressure dependence of η and the relative insensitivity of the internal rotation to pressure. Such experiments are currently underway in these laboratories.

At lower temperatures, A' , as already noted, obeys a $\tau_R \propto \eta/T$ dependence rather well. Our results on PD-Tempone in toluene and toluene-*d*₈ summarized in Figure 5 and Table IV show that typically only a fraction of this τ_R -dependent width may be attributed to intermolecular dipolar interaction of the unpaired electron with the solvent protons in protonated solvent. We discuss this point.

One can estimate the line width contribution due to this intermolecular interaction in the standard way.^{12,44} That is, with $\omega_a^2 \ll \tau^{-2} \ll \omega_e^2$ where τ is the translational diffusion correlation function

$$\tau = d^2/2D \quad (12)$$

so that pseudosecular width contributions (*i.e.*, terms in which the nuclear spin flips but the electron spin does not) are important, while nonsecular terms (*i.e.*, terms in which the electron spin flips) are unimportant, one has^{12,44}

$$T_2^{-1} = \gamma_I^2 \gamma_e^2 \hbar^2 I(I+1) [J^{(0)}(0)/6 + \frac{3}{2} J^{(1)}(\omega_a)] = \gamma_I^2 \gamma_e^2 \hbar^2 I(I+1) \frac{8\pi N}{45 dD} \quad (13)$$

where N is the density of spins d is the distance of closest approach of the interacting spins, D is the translational diffusion constant, and γ_I is the gyromagnetic ratio of the nuclei of spin I . Equation 12 is based upon the simplifying assumption that PD-Tempone and toluene have identical diffusive properties. We further assume eight spins per toluene molecule and we neglect considering their geometric

distributions within the molecule.⁴⁵ This yields $N \cong 4.5 \times 10^{22}$ spins/cm³. The result at $\tau_R = 10^{-9}$ sec, where the added contribution to A' in toluene- h_8 is ca. 0.1 G (derivative peak-to-peak width cf. Figure 5) is then $(dD) \approx 3.1 \times 10^{-15}$ cm³/sec. Use of the Stokes-Einstein relation

$$D = kT/6\pi\eta r_T \quad (14)$$

where r_T is the effective translational diffusion radius, would then give $d/r_T \approx 0.92$ Å or when eq 13 is corrected for boundary value effects,⁴⁶ $d/r_T \approx 1.15$. This result is quite reasonable in view of all the simplifying assumptions made. [In fact, if some of the T_2^{-1} contribution arises from a small isotropic hyperfine coupling with solvent protons, as is likely, then the predicted value of (dD) from eq 13 would be increased, as would the value of d/r_T from eq 14.] The main feature of this estimate, then, is that the observed difference in A' between toluene- h_8 and toluene- d_8 is of the order expected for intermolecular dipolar interactions including possible isotropic hyperfine effects. [Note that from eq 13, the perdeuterated solvent yields (1/16) the intermolecular dipolar contribution compared to the protonated solvent.]

C. Inertial Effects, and Some Other Corrections to Simple Brownian Diffusion. We have in part II discussed the ϵ parameter for PADS in terms of a very simple memory function approach. It was shown there that our empirical ϵ parameter, which is very convenient in representing the experimental results, has a simple interpretation in terms of such a memory function approach only when $\epsilon \sim 1$, which is not the case for these experiments, and this probably means a more detailed analysis of the molecular dynamics would be required. The approach in part II did not consider the matter in any further detail.

Our results in this work yield a value of $\epsilon \sim 5$ in the toluene solvents, for which the results and analysis are most reliable (and $\epsilon \sim 3$ in ethanol and acetone). (We are unable to obtain an ϵ value in the glycerol- d_3 -D₂O because decomposition of PD-Tempone occurs above 50°.) The carefully studied toluene solvent is characterized by $N \cong 1$, so anisotropic diffusion is even less likely to complicate the analysis. We have also succeeded, in the present work, in obtaining ϵ -dependent results at another frequency, viz. 35 GHz for which $\epsilon \sim 5$, implying that it is rather frequency insensitive. (More precisely, ϵ appears to have the same value for the same range of $\omega_e\tau_R$.) This value of ϵ is very similar to the value of $\epsilon \sim 4$ found for the PADS solutions. [The only substantial variation in this result for ϵ so far has been a value of $\epsilon \sim 1$ from the ¹⁷O contributions at X band for $\tau_R < 5$ psec, but for that region, the present results of Figures 4, 7, and 8 suggest other processes may begin to be important.] This apparent near constancy in ϵ is difficult to justify in terms of the simple gaussian and exponential memory functions used in part II, except in the case that only the lowest order terms are kept in a power series expansion in ω so that $\gamma'(\omega) \approx \tau_R^{-1}$ and $\gamma''(\omega) \approx \alpha\omega$ where α is a constant to be calculated from the proper molecular dynamics and $\gamma'(\omega)$ and $\gamma''(\omega)$ are the real and imaginary parts of the frequency-dependent damping coefficient. One would require that $\alpha = \epsilon^{1/2} - 1 \sim 1$ be relatively independent of solvent and temperature (but possibly a slowly varying function of τ_R).

The question naturally arises as to a physical interpretation of ϵ . One possibility, raised in part II, would be to include "short-time" inertial effects, but typical simplified expressions for $j(\omega)$ did not bear any satisfactory relation-

ship to eq 2. Use of the more complete analyses of inertial effects of Sack⁵¹ and of Hubbard⁵² (who respectively give expressions asymptotic in ω and a perturbation in the ratio $a = \tau_J/\tau_R$) does not change this conclusion.

The question of inertial effects, is, however, relevant to an analysis of our slow-tumbling model-dependent results, wherein we find good agreement with a very approximate model including substantial inertial effects, but this model yields predictions very similar to that of moderate jumps with an rms jump angle $\sim 50^\circ$. A more rigorous analysis which incorporates properly the coupling between angular momentum, orientation, and slow tumbling esr spectra has indicated that predicted slow tumbling esr line shapes are quite similar to those from the crude analysis.⁵³ Thus, it is not readily possible to distinguish between the two models (jump vs. inertial) purely from the slow-tumbling spectral simulations, and other criteria are therefore needed.

It is precisely from results in the motional narrowing region that obvious conclusions may be reached on this matter. We use Hubbard's perturbation results in $a \equiv \tau_J/\tau_R$ ^{52b}

$$j(0) = \tau_R \left[1 + \frac{11}{12} a - \frac{83}{216} a^2 + \dots \right] \quad (15)$$

where $j(0)$ replaces the expression in eq 2 for $\omega_0 = 0$. Note that the relationship of eq 10 is implied in the definition of a , so

$$a = \frac{\tau_J}{\tau_R} = \frac{I}{6kT\tau_R^2} \quad (16)$$

$a = 1.45 \times 10^{-22}(\tau_R^2 T)^{-1} \text{ sec}^2$ for PD-Tempone from eq 14. [Equation 10 is a fundamental one in the theory of rotational Brownian motion; it is required in order that an angular velocity distribution approach a Boltzmann distribution as $\tau \rightarrow \infty$.] Clearly eq 15 will not show any appreciable inertial effects unless $a \gtrsim 0.1$, which corresponds to $\tau_R \lesssim 2$ psec and $\tau_J \gtrsim 0.2$ psec (at 82° in toluene solvent). Furthermore if $\tau_R \propto \tau_J^{-1} \propto \eta/T$, then such inertial effects would according to eq 15 lead to a nonlinear dependence of $j(0)$ upon η/T . It is clear from Figure 4A, for example (where one should rigorously read $j(0)$ in place of τ_R), that a very good linear dependence upon η/T is observed over nearly the whole range studied. It is only, in fact, in the region of $\tau_R \sim 2$ psec that the τ_R (calculated from B values, see above) seems to deviate somewhat. In fact this deviation is of the correct sign and order to agree with eq 15. One must, however, recognize that the smallness in the measured value of B (as well as the various uncertainties of the analysis) in this region renders such a comparison somewhat uncertain. The main point is that the very good η/T dependence of τ_R ^{28a} is strong evidence against an important inertial component, and, as τ_R increases, inertial effects become less important. Finally, and most significantly, slow tumbling spectra show appreciable inertial effects only for $a \gtrsim 1$, but when $\tau_R \sim 10^{-8}$ sec one has from eq 16 that $\tau_J \sim 0.4 \times 10^{-16}$ sec, so a is very small indeed!

This discussion is not substantially altered, if, instead of a Brownian motion model, jump-type diffusion occurs. In this case, one must rewrite τ_R as

$$\tau_R = [6B_2R]^{-1} \quad (17)$$

where $B_2 \leq 1$ is the model parameter characteristic of the jump diffusion and discussed in detail in part I. Our slow-tumbling results imply a $B_2 \sim 0.56$ (from eq 12b of part I and an $R\tau$ value ~ 0.14). One may then show by a simple analysis that τ_J should become (cf. part II)

$$\tau_j = I/6kTB_2\tau_R \quad (18)$$

While the proper inertial corrections analogous to eq 15 have not been worked out for such a model, one notes that (1) $a \equiv \tau_j/\tau_R = I/6kTB_2\tau_R^2$ is still a small quantity and (2) inertial effects, treated as a power series in a , would still imply deviations from $j(0) \propto \eta/T$ which are not seen except perhaps for $\tau_R \lesssim 2$ psec.

It is on these grounds that we conclude a jump-type model is to be preferred to an inertial effect model in "explaining" our slow-tumbling results (but see section V). Note also that a $B_2 < 1$ would be consistent with the results for A_1^2 given in Table V, since, in general, the experimentally determined values are a little greater than those predicted from eq 9. In the case of the nonsecular spectral densities $j(\omega)$ and the associated parameter ϵ , one sees that the inertial effects would predict strongly τ_R -dependent corrections, since $a \propto \tau_R^{-1}$; again a result inconsistent with observation.

Our rejection of the importance of inertial effects over most of the range of the experiments is thus seen to be based in part upon the observed simple η/T dependence, *i.e.*, simple Stokes-Einstein behavior for τ_R . The question exists as to a mechanism that would have such a property and still lead, for example, to an $\epsilon \neq 1$. A mechanism which has been of recent theoretical concern, and is characteristic of a Brownian particle, is the backflow hydrodynamic effect, giving rise to the "long-time tails" in the correlation function (*i.e.*, the flow patterns generated by the rotating Brownian particle ultimately return to affect the particle). This effect would lead to a frequency-dependent friction coefficient $\beta(\omega)$. By an analysis outlined in Appendix B, one may write when inertial effects are unimportant that $R(\omega) \equiv kT/I\beta(\omega)$ would also be frequency dependent, *i.e.*, there is a frequency-dependent rotational diffusion coefficient: $R(\omega) \rightarrow \frac{1}{6}\gamma(\omega)$ is showing the effects of a memory function. To the extent that this applies to the backflow effect, one has in this case^{54,55}

$$\frac{1}{6}\gamma(\omega) = R(\omega) = R \left[1 - \frac{i\omega a^2/3\nu}{1 + a(-i\omega/\nu)^{1/2}} \right]^{-1} \quad (19)$$

where a is the radius of the Brownian particle and $\nu \equiv \eta/\rho$ is the kinematic viscosity with ρ the solvent density. Equation 19 has some of the correct qualitative features to explain the ϵ results: (1) $R(0) = R$, so τ_R shows simple Stokes-Einstein behavior; (2) the higher frequency spectral densities $j(\omega)$ will be the ones most significantly affected; and (3) to lowest order in the dimensionless parameter $\gamma = \omega a^2/\nu$ one has

$$R(\omega) \cong [1 - \frac{2}{3}iy]R \quad (20)$$

such that

$$\epsilon \cong [1 - (2/3)6Ra^2\rho/\eta]^2 = [1 - kT\rho/2\pi a\eta^2]^2 \quad (21)$$

and is frequency independent. (The last equality of eq 21 assumes the validity of eq 6.)

However, other considerations lead us to readily reject the importance of this mechanism. We need only note that (1) the magnitude of the correction in eq 21 is too small and of the wrong sign and (2) it is very sensitive to η/T . We estimate from eq 21 $\epsilon \sim 0.9975$ at -10° in toluene where $\eta \sim 0.1$ cP and $\tau_R = 10^{-11}$ sec, while at 100° where $\eta \sim 0.0026$ P and $\tau_R = 2 \times 10^{-12}$ sec, $\epsilon \sim 0.95$. It may be that for a small non-Brownian particle a proper theory could predict larger corrections to ϵ than given by the equations above for a Brownian particle, but our experimental results are *not*

consistent with a strong η/T dependence for ϵ , nor with the *sign* in eq 21. (Note, however, we cannot entirely rule out such considerations for anomalous behavior observed for $\tau_R \lesssim 3 \times 10^{-12}$ sec.)⁵⁶

We turn, in section V, to an analysis of our results in terms of the fluctuating torques exhibiting substantial persistence times (of the order of τ_R). This analysis seems quite effective in correlating much of our results.

V. Analysis in Terms of Fluctuating Torques

The more "traditional" analysis of the previous sections has been found to lead to several anomalies. We summarize them.

(1) The nonsecular spectral densities do not follow a Debye-type spectral density, but require the inclusion of an $\epsilon > 1$ in the manner of eq 2.

(2) As the motion approaches the slow tumbling region (*i.e.*, $10^{-10} < \tau_R < 10^{-9}$ sec), there are two types of anomalies:⁵⁷ (a) the C/B ratio becomes larger than expected; (b) the dynamic frequency shifts, particularly of the high-field line, are larger than expected.

(3) Our best model-dependent slow tumbling fits are consistent with a moderate jump model in which the rms jump angle $\langle \epsilon^2 \rangle^{1/2}$ is of the order of 50° . This appears to be an unusually large value especially when it is recognized that the jump model is based on the assumption that the duration of a jump is nearly instantaneous. Thus, another explanation in terms of the molecular dynamics might well be desirable.

We wish to show how a simple model, which includes effects of relatively slowly fluctuating torques, and inertial effects only in very lowest order, is able to give a single unified interpretation to the three classes of anomalies listed above. We present in Appendix B an outline of a derivation of a generalized rotational diffusion (or Fokker-Planck) equation which explicitly includes the fluctuating torques, in the formalism. The derivation, which takes rigorous account of the dynamical coupling between orientational, angular momentum, and anisotropic intermolecular interactions may be simplified, when inertial effects are unimportant, into a simple Brownian rotational diffusion equation in orientation space, which is just the Brownian rotation model commonly used, except now one has a frequency-dependent diffusion coefficient $R(\omega)$ [*cf.* eq B9b]. The simple assumption that the correlation function for the resultant torque experienced by the probe molecule is exponentially decaying with time constant τ_M , then leads to

$$R(\omega) = \frac{kT}{IV^2}(-i\omega + \tau_M^{-1}) \quad (22)$$

where if we let $\langle \gamma^2 \rangle^{1/2}$ be the rms torque, then

$$V^2 \equiv \langle \Upsilon^2 \rangle / IkT \quad (22a)$$

It is then an easy matter to explain anomaly (1), (*viz.* ϵ) by noting from eq B10 that the nonsecular spectral density for $L = 2$ is

$$j_2(\omega_0) = \frac{\tau_R}{1 + \epsilon\omega_0^2\tau_R^2} \quad (23)$$

but with

$$\epsilon = (1 + 6kT/IV^2)^2 \quad (24a)$$

and with

$$\tau_R \equiv \tau_M \frac{IV^2}{6kT} = \tau_M / (\sqrt{\epsilon} - 1) \quad (24b)$$

Thus our experimental results that $\epsilon \sim 4$ or 5 are equivalent

to $\tau_R \sim \tau_M$ and the rms fluctuating torque is $V\sqrt{kT} \sim \sqrt{6kT}$.

The second set of anomalies have a similar interpretation, but the spectral analysis is more complex. The width anomalies are associated with $j(\omega_\alpha) = \tau_R/[1 + \epsilon'\omega_\alpha^2\tau_R^2]$ where ω_α corresponds to hyperfine frequencies associated with a_N . However, it is clear from Table I that the anisotropic parameters such as $D^{(0)}$ and $F^{(0)}$ are of comparable magnitude, and a more careful analysis is required beyond simple relaxation theory. Such an analysis can be performed in terms of a simple perturbation treatment of the slow tumbling equations, and this is discussed in Appendix C. The main point is that the pseudosecular spectral densities refer to frequencies such as $b \pm \frac{1}{2}(F_0 + \frac{1}{2}D') = -1.2$ or $1.36 \times 10^8 \text{ sec}^{-1}$, and $b \pm \frac{1}{2}(F_0 - \frac{1}{2}D') = -1.7$ and $0.89 \times 10^8 \text{ sec}^{-1}$, while it is found that the secular spectral densities are no longer nonzero, but instead refer to frequencies such as $\frac{2}{3}(F_0 \pm D') = 0.64$ and $-0.31 \times 10^8 \text{ sec}^{-1}$. Such nonzero frequencies are usually unimportant in the fast motional region where $|F_0|, |D'| \ll \tau_R^{-1}$, but the inclusion of an $\epsilon' > 1$ into the spectral densities enhances their importance. The dynamic frequency shift corrections arise in a similar manner (*cf.* Appendix C) and are associated with spectral density terms such as $k(\omega_\alpha) = \epsilon'^{1/2}\omega_\alpha\tau_R^2/[1 + \epsilon'\omega_\alpha^2\tau_R^2]$, thus their importance is usually enhanced for $\epsilon' > 1$.

The modified equations for $T_2(M)^{-1}$ and the dynamic frequency shifts $S(M)$ are given in Appendix C. One obtains modified expressions for A, B , and C as

$$A = T_2(0)^{-1} \quad (25a)$$

$$B = \frac{1}{2}[T_2(1)^{-1} - T_2(-1)^{-1}] \quad (25b)$$

$$C = \frac{1}{2}[T_2(1)^{-1} + T_2(-1)^{-1} - 2T_2(0)^{-1}] \quad (25c)$$

Typical modified A (or A'), B , and C values are found in Figures 4 and 6 for several values of ϵ' . As already noted in section III, very good agreement for both B and C is achieved with $\epsilon' = 4$ and a proper single choice of τ_R . Note from Table III that the dynamic frequency shifts are also satisfactorily accounted for with the same value of ϵ' . We should, however, call attention to the fact that the other solvent for which very accurate measurements were obtained, *viz.* toluene, is one for which the magnetic parameters are such that the C/B ratio is not significantly affected by $\epsilon' > 1$, and the experimental result, while consistent with this, does not yield further information on this matter.⁵⁷

It should also be noted (*cf.* Figure 6C) that the value of the residual width A' can be somewhat sensitive to the analysis, *e.g.*, whether fluctuating torques are included or a conventional analysis is given. This feature of A as well as those discussed in section III tend to make the analysis of this experimental parameter more complex and less certain.

The third type of possible anomaly, that of model dependence in the slow-tumbling region can also be "explained" in similar terms. In the slow tumbling theory one requires the eigenvalues of a diffusive-type operator. The L th eigenvalue is the inverse of the exponential decay time for the L th spherical harmonic. Model dependence was introduced (*cf.* part I) in terms of the model parameter B_L such that

$$\tau_L^{-1} = B_L L(L+1)R \quad (26)$$

(note that $R \equiv (6\tau_2)^{-1}$). One particular jump model, sug-

gested by Egelstaff for simplicity, leads to (for mean jumps significantly less than π)

$$\tau_L^{-1} = L(L+1)R/[1 + R\tau_L(L+1)] \quad (27)$$

where τ is the mean time between jumps and the mean-square jump angle is equal to $6R\tau$. We now note that from eq B7 the spectral density function for the L th spherical harmonic is

$$l_L(\omega) = \frac{1}{-i\omega\sqrt{\epsilon_L'} + L(L+1)R} \quad (28)$$

where

$$\epsilon_L' = [1 + \gamma_L^2/V^2]^2 \quad (28a)$$

and γ_L is defined by eq B11c. [Note that $j(\omega) \equiv \text{Re } l(\omega)$ and $k(\omega) \equiv \text{Im } l(\omega)$]. When one Fourier-Laplace inverts eq 28 one gets

$$\epsilon_L'^{-1/2} \exp[-t/(1 + V^2/\gamma_L^2)\tau_M]$$

Thus we can define an effective decay time for the L th spherical harmonic by $\tau_{L,E}$ such that

$$\tau_{L,E}^{-1} = \tau_M^{-1}[1 + V^2/\gamma_L^2]^{-1} = \frac{\tau_M^{-1}\gamma_L^2/V^2}{1 + \gamma_L^2/V^2} \quad (29)$$

This is *identical* in form to the Egelstaff-type result of eq 27, giving the decay times for the jump model. One need only let $\gamma_2^2/V^2\tau_M = 6R = \tau_R^{-1}$ as we have done already, but also $6R\tau \rightarrow \gamma_2^2/V^2 = 6kT/IV^2$. Our experimental results compared with an Egelstaff-type model give good agreement for $R\tau \sim 0.14$ or, by this association $V^2 \sim (1/0.14)(kT/I)$ or $V\sqrt{kT} \sim \sqrt{7kT}$, which is very close to the high-temperature results obtained from ϵ and ϵ' !

An alternative way to look at this simple argument is to recognize that in the slow-tumbling region $\tau_R^{-1} \lesssim |D^{(0)}|, |F_0|$, etc. Therefore, one is interested in the higher frequency components of $\text{Re } l(\omega)$ for which the $\frac{1}{2} - \frac{1}{2}$ width of this function is just $\tau_{L,E}^{-1}$.

These simple arguments encourage us to think that the slow-tumbling model dependence may be explained in the same manner as the motional-narrowing anomalies. However, a more rigorous analysis of this matter may be carried out following the formal procedures outlined in Appendix D.

We now wish to discuss spin-rotational relaxation in terms of the slowly fluctuating torque model. We can, to a good approximation, describe spin-rotational relaxation for a spherical molecule in terms of the angular momentum correlation function $\langle J(t)J(0) \rangle$ when terms of order " a " may be neglected (*cf.* ref 52c), and " a " $\ll 1$ for our experiments. We then find that eq 9 must be replaced by

$$A^{\text{SR}} \cong [kT \sum_i (g_i - g_e)^2/3I][j_J(0) + j_J(\omega_e)] \quad (30)$$

$$W_e^{\text{SR}} \cong [kT \sum_i (g_i - g_e)^2/3I][j_J(\omega_e)] \quad (31)$$

with $j_J(\omega_e)$ given by eq B16. At first glance it appears from eq B16 and B17 that $j_J(\omega_e) \neq j_J(0)$ and $j_J(\omega_e)$ will be a complicated function of ω_e and of τ_M . However this is inconsistent with both the line width and T_1 measurements for $\tau_R < 10^{-10}$ sec. However, note first of all that for $(\omega_0\tau_M)^2 \ll 1$ eq B16 yields

$$j_J(\omega) = j_J(0) = \beta(0)^{-1} = (V^2\tau_M)^{-1} \quad (32)$$

Next we note that our above analysis yields:

$$\tau_M^{-1}\beta(0) = V^2 \approx 2.5 \times 10^{24} \gg \omega_0^2 \approx 3 \times 10^{21} \quad (33)$$

at X band ($\omega_0^2 \approx 5 \times 10^{22}$ at 35 GHz). As a result, in the region where $\omega_0^2 \tau_M^2 \gg 1$, eq B16 is easily shown to reduce again to eq 32! Finally, in the region where $\omega_0 \tau_M \sim 1$, it is true that $\beta(0) \tau_M \gg 1$, which also follows from the inequality of eq 33, and one again recovers eq 32 from eq B16. Thus *no* anomalous behavior is actually predicted for the spin-rotational relaxation. However, one must be cautious with respect to the oversimplified model utilized for discussing the fluctuating torques (*cf.* Appendix D), and a more detailed analysis could lead to a somewhat different interpretation.

Finally we wish to point out that the result $\tau_M \sim \tau_R$ is consistent with a physical model in which the fluctuating torques are due to reorientation of the solvent molecules of comparable size compared to PD-Tempone. [Such a model clearly has to be modified for PADS in ice.] Also values of rms torque of the order of $\sqrt{6}kT$ imply reasonable intermolecular interactions without any strong bonding-type intermolecular interactions.

VI. Conclusions

The PD-Tempone nitroxide radical has proved to be a very useful one for esr relaxation studies. In particular, it was possible to carefully analyze the well-resolved slow tumbling spectra in toluene- d_8 and glycerol- d_3 to demonstrate that the reorientational motion of this radical deviates significantly from that predicted for simple Brownian motion. This deviation is about the same as that previously obtained with the PADS radical. Unlike PADS, its reorientation in these solvents is found to be isotropic, and the simpler ensuing analysis leads to very good agreement between observation and the predictions from the slow-tumbling theory of Freed, *et al.* In the context of the conventional model-dependent analysis, the reorientation of this radical is best described as occurring by jumps of moderate angle (rms jump angle $\sim 50^\circ$). Again, in terms of conventional analysis, the PD-Tempone and PADS radicals show effective rotational radii significantly smaller than those estimated from X-ray results, implying reasonably large slip, but the large moment of inertia of the molecules means that the reorientation process is not significantly influenced by inertial effects. The unimportance of inertial effects is confirmed by the very good η/T dependence observed for τ_R . It is on this basis that a jump-type model is favored over a free diffusional model for explaining the slow-tumbling results in terms of previously proposed simple models.

The careful studies on PD-Tempone have confirmed that it too exhibits significant deviations of the nonsecular spectral densities from a simple Debye-like expression (represented by $\epsilon > 1$), and the anomaly is comparable to that first observed for PADS. Analysis of results at 35 GHz yielded the same deviations as X-band results. This phenomenon is not consistent with inertial contributions nor with hydrodynamic backflow effects. A related anomaly, that of the deviation of the pseudosecular and secular spectral densities from simple Debye-like expressions (represented by $\epsilon' > 1$) has been found in this work. It is most clearly seen in the glycerol solvent and probably also in ethanol. This anomaly manifests itself both in the line widths and in the dynamic frequency shifts in the region of $\tau_R \sim 10^{-9}$ sec. This anomaly, is, however, most dramatically seen in a related study of PD-Tempone in liquid crystals reported on elsewhere.

A fairly comprehensive study of the molecular dynamics

problem has been undertaken to seek to explain these anomalies. It has been found that a unified explanation for the various anomalies can be provided in terms of a dynamical model which includes slowly fluctuating random torques. Our results on ϵ and ϵ' lead to values of $\tau_m \sim \tau_R$, where τ_M is the relaxation time of the torques and an rms value for the fluctuating torques of *ca.* $\sqrt{6}kT$. It must be emphasized, however, that the analysis outlined here utilizes only the simplest possible model for the torques (*i.e.*, a single, simple exponential decay for the correlation function) and makes some simplifying approximations on their esr effects, although other aspects of the dynamics have been treated carefully. In this context it is very encouraging to note that this model of slowly fluctuating torques (including the magnitudes of the parameters) appears to be consistent with the slow-tumbling, model-dependent observations. Thus the significant deviations from Brownian motion may well be attributable to the effects of slowly fluctuating torques rather than to the notion that the molecules must jump by moderately large angles ($\sim 50^\circ$) in their reorientation. We have, in this work, also outlined how the kind of further theoretical work, which would lead to a better understanding of these physical models, may be carried out. From the experimental point of view, our study illustrates the complementary value of performing line shape and relaxation studies over the whole range from fast motional narrowing through the rigid limit. Further experimental studies to elucidate these matters are currently in progress.

In other aspects of the study, it was shown that the high-temperature W_e (from saturation studies) and residual widths A' are in good agreement with a Hubbard-type spin-rotational mechanism. The low-temperature W_e results are less readily classified, but they may well reflect spin-rotational relaxation by internal motions (by comparison with recent nmr relaxation studies). The possible effects of internal motions on W_e are probably best studied in terms of their relative insensitivity to pressure dependence. The low-temperature residual A' 's may well be due to a complex of factors including small deviations from the anisotropic rotation predicted from the C/B ratio (but within the experimental error of that analysis), intermolecular electron-nuclear dipolar interactions with solvent protons, and possibly some corrections from the fluctuating torque analysis.

Finally we note that the well-resolved rigid limit spectra allow for analysis of the complete **A** and **g** tensors, and in the case of ethanol- d_6 solvent, show the existence of two forms of the radical which are believed to be a hydrogen-bonded and a nonhydrogen bonded form.

Acknowledgments. We wish to acknowledge helpful discussions and advice from Drs. S.A. Goldman and C.F. Polnaszek.

Appendix A

We show in Figure 13 the schematics for interfacing the esr spectrometers with the PDP-9 computer.

Appendix B. Inclusion of Fluctuating Torques in the Dynamics

It is possible to construct a generalized Fokker-Planck equation for the rotational motion of a Brownian-type particle in a bath of $N + 1$ rotating particles which interact *via* pair potentials $U(\Omega_B, \Omega_i)$ and $V(\Omega_i, \Omega_j)$ that depend upon

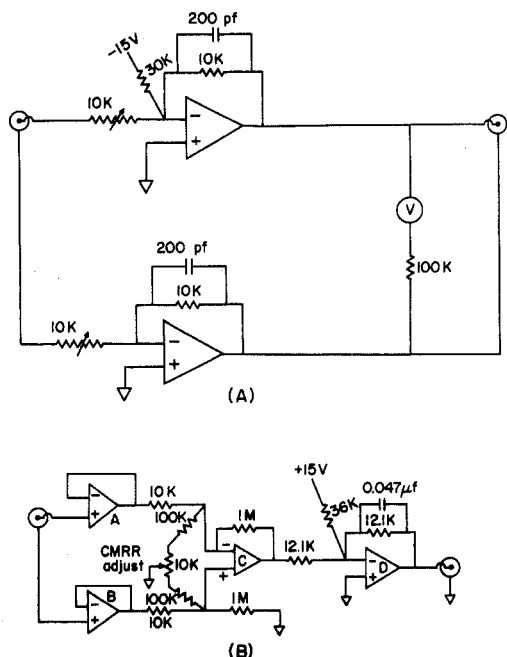


Figure 13. Schematics of the interface for the y axis from the Varian E-12 spectrometer (A) and from the Keithley Model 822 phase-sensitive detector. ∇ denotes power supply common. The operational amplifier is a Teledyne Philbrick 1026 and is operated with a floating ± 15 -V power supply (Teledyne Philbrick 2210). All BNC are floated.

orientations Ω_B and Ω_i, Ω_j for the B particle and the bath particles, respectively. This has been done⁵⁸ in a manner closely analogous to the standard treatment given for example by Resibois^{59,60} for translational motion but utilizing rotational dynamics features as discussed in part by Condiff and Dahler.⁶¹

One obtains a generalized Fokker-Planck equation for the B particle⁵⁹ of form

$$\left[\frac{\partial}{\partial t} + i\omega_B \cdot \mathbf{J}_B + \mathbf{L}_B \cdot (\nabla_L)_B + \langle \mathbf{N}_B \rangle \cdot (\nabla_L)_B \right] f_B(t) = (\nabla_L)_B \cdot \int_0^t d\tau G(t - \tau) [\omega_B/kT + (\nabla_L)_B] f_B(\tau) \quad (\text{B1})$$

In eq B1 ω_B is the angular velocity of the B particle, \mathbf{L}_B its angular momentum, $\mathbf{J}_B \equiv -i\mathbf{r}_B \times (\nabla_r)_B$, $\mathbf{L}_B \cdot (\nabla_L)_B$ is the precessional term which is identically zero for a spherical particle, and $\langle \mathbf{N}_B \rangle$ is the mean-field torque experienced by the B particle. The quantity $G(t)$ is the operator equivalent of the correlation function for the fluctuating or random torques on the B particle.⁶² The random part of the torque has a zero time average. The assumption of $G(t) = A^2\delta(t)$ yields the typical Fokker-Planck equation for rotational reorientation of a Brownian particle. When, however, a memory function such as $G(t) = A^2e^{-t/\tau_M}$, where τ_M is not extremely fast, is utilized, then a frequency-dependent frictional coefficient

$$\beta(\omega) = G(\omega)/IkT = \text{Re} \int_0^\infty e^{i\omega t} G(t) dt / IkT \quad (\text{B2})$$

is obtained. If we assume for a spherical particle that $R(0)/\beta(0) \ll 1$ where $R(0) \equiv kT/I\beta(0)$ (see below), then one expects (as discussed in section IV) that inertial effects are not directly important (*i.e.*, angular momentum relaxation occurs very rapidly), and one should be able to collapse the Fokker-Planck eq B1 in the rotational phase space of the B

particle into a Smoluchowski-type equation in just orientational space. (When $\langle \mathbf{N}_B \rangle \neq 0$, then one also requires that the orientational variation in $\langle \mathbf{N}_B \rangle$ be small compared to $I\beta^2$.) When methods similar to those utilized by Murphy and Aguirre⁶³ are employed, then one obtains a Smoluchowski-type form for eq B1:

$$\frac{\partial}{\partial t} P(t) = \int_0^t i\mathbf{J}_B \cdot \Lambda(t - \tau) \cdot (i\mathbf{J}_B - \langle \mathbf{N}_B \rangle) P(\tau) d\tau \quad (\text{B3})$$

where

$$\begin{aligned} \Lambda(\omega) &\equiv \int_0^\infty e^{i\omega t} \Lambda(t) dt \\ &= kT/I\beta(\omega) \end{aligned}$$

so that Fourier-transforming eq B3 yields

$$-P(0) - i\omega P(\omega) = i\mathbf{J}_B \cdot \frac{kT}{I\beta(\omega)} \cdot (i\mathbf{J}_B - \langle \mathbf{N}_B \rangle) P(\omega) \quad (\text{B4})$$

and a generalized Einstein relation

$$R(\omega) = kT/I\beta(\omega) \quad (\text{B5})$$

is obtained.

One may obtain the conditional probability function, or Green's function, by letting

$$\begin{aligned} P(t = 0) &= \delta(\Omega - \Omega_0) = \\ &\sum_{L,K,M} \left(\frac{2L+1}{8\pi^2} \right) \mathbf{D}_{KM}^{*L}(\Omega_0) \mathbf{D}_{KM}^L(\Omega) \quad (\text{B6}) \end{aligned}$$

In particular for the case $\langle \mathbf{N}_B \rangle = 0$, one obtains for the spherical B particle from the known properties of \mathbf{J}_B^2

$$\begin{aligned} P(\omega) &= \sum_{L,K,M} \left(\frac{2L+1}{8\pi^2} \right) \mathbf{D}_{KM}^{*L}(\Omega_0) \mathbf{D}_{KM}^L(\Omega) \times \\ &[-i\omega + L(L+1)R(\omega)]^{-1} \quad (\text{B7}) \end{aligned}$$

which is identical with the usual expressions except for the frequency-dependent diffusion coefficient $R(\omega)$. The choice of

$$G(t) = (IkT)V^2 e^{-t/\tau_M} \quad (\text{B8})$$

then yields

$$\beta(\omega) = V^2 [-i\omega + \tau_M^{-1}]^{-1} \quad (\text{B9a})$$

and

$$R(\omega) = \frac{kT}{IV^2} (-i\omega + \tau_M^{-1}) \quad (\text{B9b})$$

Thus the orientational spectral densities $j_L(\omega)$ are given by

$$\begin{aligned} j_L(\omega) &\equiv \text{Re} \int_0^\infty e^{i\omega t} \langle \mathbf{D}_{KM}^{*L}(\Omega_t) \mathbf{D}_{KM}^L(\Omega_0) \rangle dt \\ &= \frac{\tau_L}{1 + \epsilon_L \omega^2 \tau_L^2} \quad (\text{B10}) \end{aligned}$$

where

$$\epsilon_L \equiv (1 + \gamma_L^2/V^2)^2 \quad (\text{B11a})$$

$$\tau_L \equiv \tau_M V^2 / \gamma_L^2 \quad (\text{B11b})$$

$$\gamma_L^2 \equiv L(L+1)kT/I \quad (\text{B11c})$$

The Brownian motion limit is achieved by letting τ_M and $(\gamma_L/V)^2 \rightarrow 0$ while $\tau_M V^2 / \gamma_L^2$ remains finite (*i.e.*, $V^2 \tau_M \rightarrow \beta$). The dynamic frequency shift terms $k_L(\omega)$ are obtained

by taking the imaginary part of the Fourier transform in eq B10 and one gets

$$k_L(\omega) = \frac{\epsilon_L^{1/2} \omega \tau_L^2}{1 + \epsilon_L \omega^2 \tau_L^2} \quad (\text{B12})$$

One may also calculate the spectral densities for angular momentum $j_J(\omega)$. Thus for a spherical particle with $\langle \mathbf{N}_B \rangle = 0$ it follows from eq B1, B2 (as well as the treatment by Hubbard given for a frequency-independent β) that

$$j_J(\omega) = \text{Re} \int_0^\infty e^{i\omega t} g_J(t) dt \quad (\text{B13})$$

where

$$g_J(t) \equiv \langle J(t)J(0) \rangle / \langle J(0) \rangle^2 \quad (\text{B14})$$

and one may write in the usual manner for a frequency-dependent friction coefficient (cf. part II and ref 65)

$$dg_J(t)/dt = - \int_0^t \tilde{\beta}(t') g_J(t-t') dt' \quad (\text{B15})$$

where

$$\tilde{\beta}(t) = G(t)/IkT \quad (\text{B15a})$$

One then obtains from eq B13–B15 that

$$j_J(\omega) = \beta'(\omega) / \{ [\omega + \beta''(\omega)]^2 + [\beta'(\omega)]^2 \} \quad (\text{B16})$$

with

$$\beta'(\omega) \equiv \text{Re} \beta(\omega) = \beta(0) / [1 + (\omega \tau_M)^2] \quad (\text{B17a})$$

$$\beta''(\omega) \equiv \text{Im} \beta(\omega) = -\omega \tau_M \beta'(\omega) \quad (\text{B17b})$$

and

$$\beta(0) = V^2 \tau_M \quad (\text{B17c})$$

Note that if we let $\beta(0) \equiv \tau_J^{-1}$, then letting $\tau_R = \tau_L = 2$, the Hubbard relation follows from eq B11b and B17c, i.e.

$$\tau_R \tau_J = I/6kT \quad (\text{B18})$$

Equation B18 is just a special case of eq B5 for $\omega = 0$.

Appendix C. Perturbation Corrections to Line Widths and Frequency Shifts as a Function of ϵ' Near the Slow Tumbling Region

The derivation of a modified motional-narrowing line width equation to include the effects of ϵ' is performed by means of a perturbation analysis on the symmetrized form of the slow tumbling equations given in the Appendix of part I. The perturbation method for these complex symmetric matrices has already been discussed in several places.^{29,66,67}

We illustrate with the second-order coupling of the $C_{0,0}^{(2)}$ (1) contribution into the $C_{0,0}^{(0)}$ (1) term (refer to eq A1 of part I). (This latter coefficient determines the $M = +1$ or low-field line.) This contribution to $C_{0,0}^{(0)}$ (1) may be written as: $X^2/(E_0 - E_2)$ where

$$X = -(F_0 + D') \begin{pmatrix} L & 2 & L' \\ 0 & 0 & 0 \end{pmatrix}^2$$

and is the off-diagonal coupling between the $C_{0,0}^{(2)}$ (1) and $C_{0,0}^{(0)}$ (1) terms; while $E_0 \equiv (\omega - \omega_0) + 2b$ and $E_2 \equiv [(\omega - \omega_0) + 2b - \frac{2}{7}(F_0 + D')\sqrt{\epsilon'} + i\tau_R^{-1}]$ are the diagonal elements of $C_{0,0}^{(0)}$ (1) and $C_{0,0}^{(2)}$ (1), respectively, where the fluctuating torque terms have been included into E_2 in a manner such as eq D9.

Now near resonance for transition (1), we may in the mo-

tional-narrowing region let $\omega - \omega_0 + 2b \approx 0$ in the resulting expression. (When this approximation breaks down, then the line shapes will require slow-tumbling types of corrections.) This yields as the contribution $\frac{1}{5}(F_0 + D')^2 / [\frac{2}{7}(F_0 + D')\sqrt{\epsilon'} + i\tau_R^{-1}]$, the imaginary part of which contributes to the width, while the real part contributes to the dynamic frequency shift yielding an up-field shift since $F_0 + D'$ is positive [$\frac{2}{7}(F_0 + D') \sim 6.4 \times 10^7 \text{ sec}^{-1}$ or 3.6 G].

It should be noted that such contributions are automatically included in a slow tumbling program provided either $\epsilon' = 1$ or else the effects of fluctuating torques are adequately included.

In the presence of asymmetric parameters (i.e., $F_2 \neq 0$ and/or $D^{(2)} \neq 0$), then to avoid some complicating features in the perturbation analysis we assume either (1) $|F_2|$ and $|D^{(2)}|$ are small compared to $|F_0|$ and $|D^{(0)}|$, respectively, or else (2) the motion is anisotropic enough that $|\tau(0) - \tau(2)| \gg |F_2|, |D^{(2)}|$. (In the absence of both conditions, then there are some accidental "degeneracies.") The generalization of eq 5 of part I to the present problem is then found to be

$$\begin{aligned} T_2(M)^{-1} \cong & \frac{4\pi^2}{5} \xi^2 \left(D^{(0)^2} \left\{ \frac{8}{3} j_M^0(0) M^2 + j_M^0(4,5) (\delta_{M,1} + \right. \right. \\ & \delta_{M,0}) + j_M^0(6,7) (\delta_{M,0} + \delta_{M,-1}) + \left. \left. \left[\frac{14}{3} - \frac{1}{3} (\delta_{M,1} + \right. \right. \right. \\ & \left. \left. \left. \delta_{M,-1}) \right] j^0(\omega_e) \right\} + 2(D^{(2)})^2 \left\{ \frac{8}{3} j_M^2(0) M^2 + j_M^2(4,5) (\delta_{M,1} + \right. \right. \\ & \delta_{M,0}) + j_M^2(6,7) (\delta_{M,0} + \delta_{M,-1}) + \left. \left. \left[\frac{14}{3} - \frac{1}{3} (\delta_{M,1} + \right. \right. \right. \\ & \left. \left. \left. \delta_{M,-1}) \right] j^2(\omega_e) \right\} + \frac{\pi}{10} \omega_0 \xi M \left(D^{(0)} g^{(0)} \left\{ \frac{16}{3} j_M^0(0) + \right. \right. \right. \\ & \left. \left. \left. 4j^0(\omega_e) \right\} + 2D^{(2)} g^{(2)} \left\{ \frac{16}{3} j_M^2(0) + 4j^2(\omega_e) \right\} \right) + \\ & \frac{\omega_0^2}{80} \left((g^{(0)})^2 \left\{ \frac{8}{3} j_M^0(0) + 2j^0(\omega_e) \right\} + \right. \\ & \left. \left. 2(g^{(2)})^2 \left\{ \frac{8}{3} j_M^2(0) + 2j^2(\omega_e) \right\} \right) \right) \quad (\text{C1}) \end{aligned}$$

where

$$\begin{aligned} j_M^K(i) &= \tau(K) / [1 + \epsilon' \tau(K)^2 \omega_e^K (i)^2] \\ i &= 0; 4,5; \text{ or } 6,7 \quad K = 0 \text{ or } 2 \quad (\text{C2}) \end{aligned}$$

and

$$\omega_M^0(0) = -\omega_M^2(0) = \frac{2}{7}(F_0 + MD') \quad (\text{C3a})$$

$$\begin{aligned} \omega_M^K(4,5) &= (-1)^{M+1} b + (-1)^{K/2} \frac{1}{7}(F_0 + \frac{1}{2} D') \\ M &= 0 \text{ or } 1 \quad K = 0 \text{ or } 2 \quad (\text{C3b}) \end{aligned}$$

$$\begin{aligned} \omega_M^K(6,7) &= (-1)^M b + (-1)^{K/2} \frac{1}{7}(F_0 - \frac{1}{2} D') \\ M &= 0 \text{ or } 1 \quad K = 0 \text{ or } 2 \quad (\text{C3c}) \end{aligned}$$

Also

$$j^K(\omega_e) = \tau(K) / [1 + \epsilon' \tau(K)^2 \omega_e^2] \quad (\text{C4})$$

and $\delta_{M,0}$, etc. are Kroenecker delta functions. The notation is otherwise identical with that of part I.

The dynamic frequency shifts $S(M)$ are obtained from a modified form of eq C1. One first relates each $j_M^K(i)$ in eq C1 by $k_M^K(i)$ where

$$k_M^K(i) \equiv \epsilon'^{1/2}(-1)\omega_M^K(i)j_M^K(i) \quad (\text{C5a})$$

while $j^K(\omega_e)$ is replaced by

$$k^K(\omega_e) \equiv \epsilon'^{1/2}\omega_e j^K(\omega_e) \quad (\text{C5b})$$

Then the resulting expression is set equal to $S(M)$ the dynamic frequency shift of the M th line.

When $\epsilon'\tau(K)^2\omega_M^K(i)^2 \ll 1$ then $j_M^K(i)$ may be approximated as

$$j_M^K(i) \cong \tau(K)[1 - \epsilon'\tau(K)^2\omega_M^K(i)^2]$$

and this may be used to simplify the analysis.

Appendix D. Generalizing the Stochastic Liouville Equation

(1) *Time-Dependent Stochastic-Liouville Equation.* It is possible to explicitly include the spin-Liouville operator \mathfrak{H}_s^X into the analysis of the rotational motion given in Appendix B, and this leads to the form for the spin density matrix ρ_B for the B particle^{58,68}

$$\dot{\rho}_B(t) = -i\mathfrak{H}_s^X(\Omega_B)\rho_B(t) - \int_0^t \Gamma(t-\tau)\rho_B(\tau) d\tau \quad (\text{D1})$$

where

$$\Gamma(t-\tau) \equiv [\omega_B \cdot \mathbf{J}_B + \tilde{\mathbf{L}}_B \cdot (\nabla_L)_B + (\mathbf{N}_B) \cdot (\nabla_L)_B] \delta(t-\tau) - (\nabla_L)_B \cdot G(t-\tau) e^{-i\mathfrak{H}_s^X(t-\tau)} \cdot \left[\frac{\omega_B}{kT} + (\nabla_L)_B \right] \quad (\text{D1a})$$

The Fourier-Laplace transform of eq D1 yields

$$\rho(\omega) = [-i\omega + i\mathfrak{H}_s^X + \Gamma(\omega)]^{-1} \rho(t=0) \quad (\text{D2})$$

[For simplicity we have neglected any noncommutation of bath and spin variables in these expressions (although it is not necessary),⁶⁹ *i.e.*, this is a high-temperature approximation.] It is, of course, then possible to collapse the dependence upon \mathbf{L}_B as before to obtain a result for $\Gamma(\omega)$ analogous to eq B4 (*i.e.*, a generalized Smoluchowski form). One merely uses in eq B4 the expression

$$\beta(\omega - \mathfrak{H}_s^X) = V^2[-i(\omega - \mathfrak{H}_s^X) + \tau_M^{-1}]^{-1} \quad (\text{D2a})$$

in place of eq B9a. One may then solve this expression for predicting slow-tumbling experiments. However, because of the frequency-dependence of $\Gamma(\omega)$ one may not, in general, solve for the spectrum by only a single diagonalization, *cf.* parts I and II.

(2) *Augmented Stochastic-Liouville Equation.* The conventional formalism of the stochastic-Liouville equation requires the use of a Markovian time-independent operator Γ .^{29,32a} A stochastic assumption for the torques (*e.g.*, $G(t) = \Upsilon^2 e^{-t/\tau_M}$), may, in the context of the standard stochastic-Liouville approach, be obtained by augmenting the Γ operator, used by Bruno and Freed⁵³ to discuss inertial effects to explicitly include a dynamical coupling to the fluctuating torques plus a stochastic model for the relaxation of these torques (*e.g.*, a diffusion of the orientation of the resultant instantaneous torque in the unit sphere).

Such an augmented stochastic-Liouville equation will be time independent and can be effectively used to analyze slow-tumbling spectra by a straightforward generalization of the procedures of Bruno and Freed.⁵³ We illustrate with a very crude example, which, however, is seen to reduce essentially to give the spectral densities of eq B10.

We are primarily concerned with the limit when inertial

effects are unimportant, *i.e.*, $R/\beta = kT/I\beta^2 \ll 1$. In this limit we wish only to solve to lowest order in R/β . In this limit (and only in this limit) the inertial problem, as discussed by Bruno and Freed,⁵³ may be satisfactorily approximated in a quasi-one-dimensional sense. Then, in the Brownian motion limit, for which $\tau_M \rightarrow 0$ ⁵³

$$\Gamma \longrightarrow iv|j_u^2|^{1/2} - \beta \left(\frac{\partial}{\partial v} v + \frac{kT}{I} \frac{\partial^2}{\partial v^2} \right) \quad (\text{D3})$$

where

$$|j_u^2|^{1/2} \mathcal{D}_{kM}^L(\Omega) \equiv [L(L+1)]^{1/2} \mathcal{D}_{kM}^L(\Omega)$$

and v is the magnitude of the angular momentum. For simplicity of presentation, we only consider spherical symmetry, so $K = M = 0$ and we neglect these "quantum numbers." One can then solve for $P(\Omega, v, t)$ in terms of the appropriate eigenfunction expansion, in which the Hilbert space of v is spanned by the Hermite functions $h_n(v)$, while the needed orientation space is spanned by $\mathcal{D}_{00}^L(\Omega)$. Then the coefficients $a_{L,n}$ in such an expansion obey the algebraic equation (*cf.* ref 53, eq 34)

$$[(\omega - \omega_0) - in\beta]a_{L,n} + (\sqrt{n+1} a_{L,n+1} + \sqrt{n} a_{L,n-1})\gamma_L = \delta_{n,0} \quad (\text{D4})$$

where γ_L is defined by eq B11c. Since $\beta/\gamma_L \ll 1$, perturbation techniques allow one to solve for $a_{L,0}$ in terms of only the coupling to the $n = 1$ coefficient.

We now introduce the fluctuating torque as an extra degree of freedom, but in a very crude manner to obtain the augmented stochastic-Liouville equation

$$[(\omega - \omega_0) - iE_m]a_{L,n,m} + \gamma_L(\sqrt{n+1} a_{L,n+1,m} + \sqrt{n} a_{L,n-1,m}) + V[\sqrt{n}\sqrt{m+1} a_{L,n-1,m+1} + \sqrt{n+1}\sqrt{m} a_{L,n+1,m-1}] = \delta_{n,0}\delta_{m,0} \quad (\text{D5})$$

where $m = 0$ or 1 and $E_m = m\tau_M^{-1}$. This corresponds to a model in which the reduced torque V fluctuates between the two values $\pm V$ with mean lifetime in each state of $2\tau_M$. For $|V\tau_M| \ll 1$, eq D4 is easily recovered from eq D5 with the understanding that $a_{L,n,0} \rightarrow a_{L,n}$, and $\beta \equiv V^2\tau_M$. The form of the term in V has been chosen in recognition of the fact that the torque acts to change the angular momentum (*cf.* eq B1), and any dependence of the torque upon orientation of the molecule is neglected for simplicity. Again, in the spirit of simplicity we only consider terms to lowest order in γ_L . Then in this limit eq D5 is simply for $a_{L,0,0}$

$$ia_{L,0,0} = \{i\Delta\omega + \gamma_L^2[i\Delta\omega + V^2/(i\Delta\omega + \tau_M^{-1})]\}^{-1} = [i\Delta\omega(1 - \gamma_L^2/Q + \gamma_L^2\beta j_T/Q) + \gamma_L^2 V^2 j_T/Q]^{-1} \quad (\text{D6})$$

where

$$j_T \equiv \tau_M/(1 + \Delta\omega^2\tau_M^2) \quad (\text{D7a})$$

and

$$Q \equiv \Delta\omega^2[1 - \beta j_T]^2 + V^4 j_T^2 \quad (\text{D7b})$$

In the Brownian limit of $\tau_M \rightarrow 0$, but with $V^2\tau_M \equiv \beta$ remaining finite, $Q \rightarrow \Delta\omega^2 + \beta^2$ and

$$ia_{L,0,0} \longrightarrow \left[i\Delta\omega \left(1 - \frac{\tau_L^{-1}/\beta}{1 + \Delta\omega^2\beta^2} \right) + \tau_L^{-1}/(1 + \Delta\omega^2/\beta^2) \right]^{-1} \quad (\text{D8})$$

with τ_L defined by eq B11b. Equation D8 only includes the frequency-dependent inertial correction to very lowest

order in $\alpha = \tau_L^{-1}/\beta$. However in the limit of slow τ_M , more precisely $\beta j_T \gg 1$, one gets $Q \rightarrow \beta^2 j_T / \tau_M$ and

$$i a_{L,0,0} \rightarrow \left[i \Delta \omega \left(1 + \frac{\tau_M}{\tau_L} \right) + \tau_L^{-1} \right]^{-1} \quad (\text{D9})$$

which is the same result as eq B10.

The augmented Γ of eq D5 may now be utilized in the stochastic Liouville equation

$$\dot{\rho} = -i \tilde{\mathcal{L}}_s^x(\Omega) \rho - \Gamma \rho$$

and the problem solved in the manner of Bruno and Freed.⁵³

It is interesting to note that from the point of view of the augmented stochastic-Liouville approach some physically significant weaknesses of eq D5 are readily exhibited, and since the approach is nearly equivalent in its results to that of eq B4 and B8, it should be true of that approach as well. They are (1) when $|V\tau_M|^2 \gg 1$ (as is the case for the experiments described here), then simple relaxation arguments do not apply, *i.e.*, there is a "slow-tumbling" condition with respect to the fluctuating torques. Thus a better dynamical description would more properly allow for the long persistence of the torques (*e.g.*, one may let $n = 0, 1, 2, \dots$ etc. in eq D5 corresponding to a continuous range of V and a slow motional condition which brings in a whole range of the different relaxation modes corresponding to the different m values; this is formally analogous to the inertial effect problem of eq D4 and discussed in detail by Bruno and Freed). Also (2) the dependence of the fluctuating torques on the orientation of the B particle relative to the instantaneous equilibrium position has been ignored. This is a very important consideration, and furthermore provides a mechanism for quenching the fluctuating torque by reorientation of the B particle. This would, in part, remove the difficulty (1). Then (3): the higher order mixing of inertial and torque terms when $V \lesssim \gamma_L$ has been neglected in going from eq D5 to D6, but a proper analysis of such effects would probably require the correct three-dimensional model for the angular momentum (*cf.* ref 53).

These important considerations will be discussed in detail elsewhere, but they emphasize the limitations of the simple models.

References and Notes

- (1) A preliminary account of this work was given at the Varian Workshop, Vanderbilt University, June 1973. Supported in part by grants from the National Science Foundation (Grant No. GP-13780), the Donors of the Petroleum Research Fund, administered by the American Chemical Society, and by the Cornell University Materials Science Center.
- (2) (a) Part I: S. A. Goldman, G. V. Bruno, C. F. Polnaszek, and J. H. Freed, *J. Chem. Phys.*, **56**, 716 (1972); (b) part II: S. A. Goldman, G. V. Bruno, and J. H. Freed, *ibid.*, **59**, 3071 (1973).
- (3) G. Poggi and C. S. Johnson, Jr., *J. Magn. Resonance*, **3**, 436 (1970).
- (4) E. G. Rozantsev, "Free Nitroxyl Radicals," Plenum Press, New York, N.Y., 1970.
- (5) C. Jolicoeur and H. L. Friedman, *Ber. Bunsenges. Phys. Chem.*, **75**, 248 (1971).
- (6) A. M. Wasserman, A. M. Kuznetsov, A. L. Kovarskii, and A. L. Buchachenko, *Zh. Strukt. Khim.*, **12**, 609 (1971).
- (7) R. P. Shibaeva, L. O. Atovmyan, M. G. Neiganz, L. A. Novakovskaya, and S. L. Ginzburg, *Zh. Strukt. Khim.*, **13**, 42 (1972).
- (8) (a) G. F. Hatch and R. W. Kreilick, *J. Chem. Phys.*, **57**, 3696 (1972); (b) R. W. Kreilick, *ibid.*, **46**, 4260 (1967).
- (9) T. E. Gough and F. W. Grossman, *J. Magn. Resonance*, **7**, 24 (1972).
- (10) J. I. Smith, "Modern Operational Circuit Design," Wiley-Interscience, New York, N.Y., 1971, p 132.
- (11) A. Savitzky and M. J. E. Golay, *Anal. Chem.*, **36**, 1627 (1964).
- (12) M. P. Eastman, R. G. Kooser, M. R. Das, and J. H. Freed, *J. Chem. Phys.*, **51**, 2690 (1969).
- (13) J. C. Lang and J. H. Freed, *J. Chem. Phys.*, **56**, 4103 (1972).
- (14) A. J. Barlow, J. Lamb, and A. J. Matheson, *Proc. Roy Soc., Ser. A*, **292**, 322 (1966).
- (15) "Handbook of Chemistry and Physics," C. D. Hodgman, Ed., Chemical Rubber Publishing Co., Cleveland, Ohio, 1962.
- (16) A. H. Reddoch, *J. Chem. Phys.*, **43**, 225 (1965).
- (17) A. S. Kabankin, G. M. Zhidomirov, and A. L. Buchachenko, *J. Magn. Resonance*, **9**, 199 (1973).
- (18) I. Morishima, K. Endo, and T. Yonezawa, *J. Chem. Phys.*, **58**, 3146 (1973).
- (19) N. A. Sysoeva and A. L. Buchachenko, *Zh. Strukt. Khim.*, **13**, 42 (1972).
- (20) V. P. Gollkov and V. I. Muromtsev, *Zh. Strukt. Khim.*, **13**, 332 (1972).
- (21) (a) A. Abragam, "The Principles of Nuclear Magnetic Resonance," Oxford University Press, London, 1961, Chapter IV; (b) R. P. Mason and J. H. Freed, *J. Phys. Chem.*, **78**, 1321 (1974).
- (22) C. F. Polnaszek and J. H. Freed, to be submitted for publication.
- (23) C. F. Polnaszek, Ph.D. Thesis, Cornell University, Ithaca, N.Y., 1974.
- (24) G. S. Owen and G. Vincow, *J. Chem. Phys.*, **54**, 368 (1971).
- (25) R. G. Kooser, W. V. Volland, and J. H. Freed, *J. Chem. Phys.*, **50**, 5243 (1969).
- (26) J. H. Freed and G. K. Fraenkel, *J. Chem. Phys.*, **39**, 326 (1963).
- (27) Second line from top, $\tau(0)$ in $(D^{(2)})^2 \tau(0)$ should be $\tau(2)$.
- (28) (a) It is known, *cf.* ref 14, that $\ln \eta$ for toluene does not follow a simple Arrhenius dependence upon $1/T$, but shows some deviations. Our results for τ_R show a better linear dependence when plotted vs. η/T than when plotted as $\ln \tau_R$ vs. $1/T$. (b) Since, for X band, the g tensor contributions to A are small, then the dependence of A upon hyperfine tensor A is nearly the same as that for c upon A (*cf.* eq 5 of part I). Therefore any uncertainty in A would have no appreciable effect on the predicted A/C ratio, and since τ_R is obtained from equating experimental and theoretical values of C , neither would it have any appreciable effect on the experimental vs. calculated ratio of A . This is no longer true for 35 GHz, where the g tensor contribution to A is about $\frac{2}{3}$ of the total calculated value. (Note that in I, a single temperature measurement of A at 35 GHz led to a result that A' was the same for the PADS-glycerol-H₂O system at X and R bands, but that result was probably less well defined and involving more solvent interaction than the present work).
- (29) J. H. Freed, G. V. Bruno, and C. F. Polnaszek, *J. Phys. Chem.*, **75**, 3385 (1971).
- (30) G. K. Fraenkel, *J. Chem. Phys.*, **42**, 4275 (1965).
- (31) J. H. Freed, *J. Chem. Phys.*, **49**, 376 (1968).
- (32) (a) J. H. Freed in "Electron Spin Relaxation in Liquids," L. T. Muus and P. W. Atkins, Ed., Plenum Press, New York, N.Y., 1972, Chapter VIII. (b) It should be noted, that for $\tau_R = 3.2 \times 10^{-10}$ sec, when only nonsecular static and dynamic frequency shifts contribute and the pseudosecular and secular contributions are negligible, that there is a small systematic discrepancy between prediction and experiment that is mainly in the apparent splitting between the low-field and center lines. This discrepancy could qualitatively be explained as due to a large increase in the contribution of the nonsecular dynamic but not static frequency shift contributions, but quantitatively it would have to be greater by a factor of 80 than predicted for $\epsilon = 1$. However this discrepancy has only a small effect on the analysis of the large pseudosecular and secular contributions for the slower motions.
- (33) M. Huisjen and J. S. Hyde, *J. Chem. Phys.*, **60**, 1682 (1974).
- (34) J. S. Hyde, J. C. W. Chien, and J. H. Freed, *J. Chem. Phys.*, **48**, 4211 (1968).
- (35) M. P. Eastman, G. V. Bruno, and J. H. Freed, *J. Chem. Phys.*, **52**, 321 (1970).
- (36) J. S. Hwang, D. Kivelson, and W. Plachy, *J. Chem. Phys.*, **58**, 1753 (1973).
- (37) R. A. Howie, L. S. D. Glasser, and W. Moser, *J. Chem. Soc. A*, 3043 (1968).
- (38) J. H. Freed, *J. Chem. Phys.*, **41**, 2077 (1964).
- (39) R. E. D. McClung and D. Kivelson, *J. Chem. Phys.*, **49**, 3380 (1968).
- (40) W. Z. Plachy, Ph.D. Thesis, UCLA, 1967.
- (41) G. R. Luckhurst and J. N. Ockwell, *Mol. Phys.*, **16**, 165 (1969).
- (42) P. W. Atkins in "Electron Spin Relaxation in Liquids," L. T. Muus and P. W. Atkins, Ed., Plenum Press, New York, N.Y., 1972.
- (43) P. S. Hubbard, *Phys. Rev.*, **131**, 1115 (1963).
- (44) Reference 21, Chapter VIII.
- (45) P. S. Hubbard, *Phys. Rev.*, **131**, 27 (1963).
- (46) Equation 13 is based upon the usual relative translational diffusion model,⁴⁴ which, however, neglects the reflecting boundary at $r = d$ in the solution to the diffusion equation (although the spectral densities are then calculated from $r = d$ to $r \rightarrow \infty$). A proper analysis, including the boundary effects (J. H. Freed, unpublished) shows that the factor of $\frac{2}{15}$ in eq 13 should become very nearly $\frac{1}{6}$. The boundary-value effects have more serious consequences for the nonzero frequency spectral densities (J. H. Freed, unpublished). In this connection we note that for $\tau_R \sim 10^{-9}$ sec, if a Stokes-Einstein relation applies and $d = 2r_0$ so that $\tau = 9\tau_R$ (*cf.* ref 44), that the condition $\omega_a^2 \approx (1.28 \times 10^8 \text{ sec}^{-1})^2 \ll \tau^{-2}$ is no longer fulfilled, and one must correct the spectral densities for the pseudosecular frequencies arising from $S_{z\pm}$. Other corrections analogous to those discussed in section V may also be called for.
- (47) R. Wilson and D. Kivelson, *J. Chem. Phys.*, **44**, 154 (1966).
- (48) An analysis of eq 5 of part I shows that the pseudosecular and nonsecular contributions from A do make an important contribution to A and these have been removed in converting A to A' . Any errors in the analysis of τ_R , N , or of the parameter ϵ' could influence our result. It would, however, also result in an error in the g -tensor contribution, which should have been reflected in the 35-GHz results.
- (49) J. Jonas, *Advan. Magn. Resonance*, **6**, 73 (1973).
- (50) In this connection, one notes the high-temperature anomaly in the pa-

parameter C , most clearly seen in Figure 4A for toluene, but also evident in Figures 7B and 8B for ethanol and acetone, is characterized by a small but essentially η/T independent value. It may well be that this represents some intramolecular process which weakly modulates the hyperfine interaction. The interconversion between the two equivalent twisted boat conformations would not in itself modulate a_N unless the related vibrational or torsional motion leads to some probability between the two equilibrium conformers.

- (51) R. A. Sack, *Proc. Phys. Soc.*, **76**, 402, 414 (1957).
 (52) (a) P. S. Hubbard, *Phys. Rev. A*, **6**, 2421 (1972); (b) **8**, 1429 (1973), (c) **9**, 481 (1974).
 (53) G. V. Bruno and J. H. Freed, *J. Phys. Chem.*, **78**, 935 (1974).
 (54) L. D. Landau and E. M. Lifshitz, "Fluid Mechanics," Pergamon Press, London, 1959, p 97.
 (55) E. Hange and A. Martin-Löf, *J. Stat. Phys.*, **7**, 259 (1973).
 (56) In any esr line width study, one must be concerned with the possibility of contributions from modulation of the isotropic hyperfine interaction. Thus, for example, the two values of $\langle a \rangle$ obtained from the rigid limit simulations in ethanol- d_6 solvent are $a_I = 15.43$ G and $a_{II} = 14.68$ G. One must then add to the coefficient of M^2 in the line width eq 5 of I the term: $\tau_0 \rho_I \rho_{II} \gamma_e^2 (a_I - a_{II})^2 [1 - (\frac{1}{2})(1 + \omega_0^2 \tau_0^2)^{-1}]$ where $\tau_0 = \tau_I \tau_{II} / (\tau_I + \tau_{II})$ with τ_I and τ_{II} as the lifetimes in the two states. For the above values of a_I and a_{II} , and for $\rho_I \sim \rho_{II} \sim \frac{1}{2}$, one gets $f(0)/\tau_0 \sim 4.36 \times 10^{13} \text{ sec}^{-2}$. One would need τ_0 to be about 200 times slower than τ_R , with the same η/T dependence, in order to predict significant errors (of ca. factors of 2) in the estimates of τ_R in an effort to explain an $\epsilon > 1$. It is not likely that a given H-bonded state persists so long in glycerol water (for PADS), nor is it likely to expect similar solvation effects in toluene solvents for uncharged PD-Tempone even though in both cases $\epsilon \sim 5$. [Note that there would also be a contribution to the coefficient of M of $\tau_0 \rho_I \rho_{II} \gamma_e \beta_e / h (a_I - a_{II})(g_I - g_{II})$.] The anisotropic terms of eq 5 of I would also have to be modified as shown by Freed and Fraenkel,²⁸ but since these are small corrections and the effective $\tau^{-1} = \tau_R^{-1} + \tau_0^{-1} \geq \tau_R^{-1}$, they would certainly have a negligible effect. [Note in the case of anisotropic terms, interconversion between the two twisted boat conformations would be another mechanism, but (1) it would only tend to average a small fraction of the anisotropic parameters, so similar arguments would indicate its effects are negligible, and (2) it should be much less sensitive to η/T than is τ_R .] See also ref 50.
 (57) Anomalies 2a and 2b have been found to be more dramatic in a related study of PD-Tempone in nematic liquid crystals (cf. ref 22,23). This per-

haps emphasizes the important role played by the fluctuating torques.

- (58) L. P. Hwang and J. H. Freed, to be submitted for publication.
 (59) P. M. Resibois, "Electrolyte Theory," Harper and Row, New York, N.Y., 1968, Chapter IV.
 (60) J. Albers, J. M. Deutch, and I. Oppenheim, *J. Chem. Phys.*, **54**, 3541 (1971), also give a related treatment, but for Brownian translational motion of a large particle.
 (61) D. W. Condiff and J. S. Dahler, *J. Chem. Phys.*, **44**, 3988 (1966).
 (62) This random torque operator correlation function is explicitly defined by

$$G(t) \equiv \int \prod_i d\Gamma_i (\mathbf{N}_B - \langle \mathbf{N}_B \rangle) e^{-t(1-\hat{P})L(t)} (\mathbf{N}_B - \langle \mathbf{N}_B \rangle) \rho^f$$

where L is the Liouville operator for the $N+1$ particles, ρ^f the equilibrium distribution of the N bath particles, the integration is over the rotational phase space of these bath particles, \mathbf{N}_B is the instantaneous torque on the B particle, and P is the usual projection operator defined equivalently to eq IV 99 of ref 59.

- (63) T. J. Murphy and J. L. Aguirre, *J. Chem. Phys.*, **57**, 2098 (1972).
 (64) This form of $f_L(\omega)$ is similar to a result of D. Kivelson and T. Keyes [*J. Chem. Phys.*, **57**, 4599 (1972)] obtained from a simplified analysis of the dynamics (based on the Mori method) in terms of convenient "pseudovariables" for what they call the SLOR-WAIL limit. While the results are similar we note that (1) the analysis outlined here is based on a more complete treatment of the true dynamical variables, the true physical meaning of the "pseudovariables" being somewhat unclear; and (2) the similarity of the results is only achieved because (a) angular momentum relaxation is taken as very rapid and inertial effects are unimportant and (b) the very simple form eq B8 for $G(t)$ has been used here.
 (65) R. Kubo, *Rep. Progr. Phys.*, **29**, 255 (1966).
 (66) C. F. Polnaszek, G. V. Bruno, and J. H. Freed, *J. Chem. Phys.*, **58**, 3185 (1973).
 (67) J. H. Freed, *J. Phys. Chem.*, **78**, 11t5 (1974).
 (68) This form for a time-dependent stochastic-Liouville equation was suggested in a related context, cf. J. H. Freed, ref 32 Chapter IX.
 (69) When this commutation is not neglected, then one must replace $G(t)e^{-i\mathcal{H}_0 t}$ in eq D2 by:

$$G_{\text{new}}(t) \equiv \int \prod_i d\Gamma_i (\mathbf{N}_B - \langle \mathbf{N}_B \rangle) \exp[-t(1-\hat{P})L t - i\mathcal{H}_0 X t] (\mathbf{N}_B - \langle \mathbf{N}_B \rangle) \rho^f$$

cf. ref 62.